Lithos 318–319 (2018) 244–266

Contents lists available at ScienceDirect

Lithos

journal homepage: www.elsevier.com/locate/lithos

U-Pb ages of detrital zircons from the Internal Betics: A key to deciphering paleogeographic provenance and tectono-stratigraphic evolution

Antonio Jabaloy-Sánchez [a,*], Cristina Talavera [b,c], María Teresa Gómez-Pugnaire [d], Vicente López-Sánchez-Vizcaíno [e], Mercedes Vázquez-Vílchez [f], Martín Jesús Rodríguez-Peces [g], Noreen Joyce Evans [c]

[a] Departamento de Geodinámica, Universidad de Granada, 18002 Granada, Spain
[b] School of Geosciences, University of Edinburgh, The King's Building, James Hutton Road, EH9 3FE Edinburgh, UK
[c] School of Earth and Planetary Science, John de Laeter Center, Curtin University, Bentley 6845, Australia
[d] Departamento de Mineralogía y Petrología, Universidad de Granada, 18002 Granada, Spain
[e] Departamento de Geología, Universidad de Jaén, Jaén, Spain
[f] Departamento de Física de la Materia Condensada, Cristalografía y Mineralogía, Facultad de Ciencias, Universidad de Valladolid, C/ Paseo de Belén, 7, 47011 Valladolid, Spain
[g] Departamento de Geodinamica, Estratigrafía y Paleontología, Universidad Complutense de Madrid, Madrid, Spain

ARTICLE INFO

Article history:
Received 14 May 2018
Accepted 26 July 2018
Available online 4 August 2018

Keywords:
Detrital zircon ages
Nevado-Filábride Complex
Cantabrian Zone
South Iberian paleomargin
Alborán Domain

ABSTRACT

Zircons from the Nevado-Filábride Complex metamorphic rocks yielded 891 concordant inherited detrital ages. The 342 concordant ages from the Aulago Fm indicate a Pennsylvanian maximum depositional age, while the age density distribution indicates that this formation is closely related to the Cantabrian Zone (north of the Iberian Massif). The dominant Ediacaran and Cryogenian populations, at ca. 596 and 788 Ma respectively, relate the Nevado-Filábride Complex to northern Gondwana terranes. A discrete Mesoproterozoic zircon population at ca. 1031 Ma (Tonian-Late Estenian population) suggests that the basement of the Nevado-Filábride Complex could have been located near of the Saharan Metacraton and west of the East African Orogen at the beginning of the Paleozoic. The 549 concordant ages from the Tahal Fm yield an Early Permian age for the protoliths. The age density distribution pattern records erosion of rocks from the Variscan belt, including Late-Variscan magmatic rocks. Zircon spectra differ from those of the Alborán Domain, supporting the hypothesis that the Nevado-Filábride Complex is part of the South Iberian Domain. Furthermore, data from the Tahal Fm are similar to those of Permo-Triassic rocks from the Iberian Ranges.

1. Introduction

The Betic Cordillera, together with the Rif belt in Morocco (Fig. 1), constitutes the western end of the Western Alpine Mediterranean orogen and can provide insights into its evolution. However, the geodynamic evolution of the Betic Cordillera is under debate given observed discrepancies in Paleozoic and Mesozoic paleogeographic reconstructions (i.e. Esteban et al., 2017; Gómez-Pugnaire et al., 2012; Platt et al., 2013; Rodriguez-Cañero et al., 2018). The controversy essentially arises from different interpretations of the relative location and origin of continental fragments formed during the opening and evolution of the Rheic, Paleotethys, and Neothetys oceans. Resolution of the issues is further complicated by intense metamorphic and deformational overprinting during the Alpine orogeny, mainly in the Internal zones of the Western Mediterranean mountain belts.

The Alborán Domain (Fig. 1) was defined by Balanyá and García-Dueñas (1987) and originally included three metamorphic complexes that were, from bottom to top, the Nevado-Filábride Complex (NFC), Alpujárride Complex (AC) and Maláguide Complex (MC) (Fig. 1). The Alborán Domain has recently been redefined and it now comprises only the two upper tectonic complexes: the AC below and the MC on top (Behr and Platt, 2012; Booth-Rea et al., 2007; Gómez-Pugnaire et al., 2012; Platt et al., 2013; Rodriguez-Cañero et al., 2018). At present, the NFC (Fig. 2) is considered to be part of the southern paleomargin of the Iberian Massif that was subducted below the Alborán Domain (Behr and Platt, 2012; Booth-Rea et al., 2007; Gómez-Pugnaire et al., 2012; Platt et al., 2013; Rodriguez-Cañero et al., 2018). In addition, the location and evolution of the redefined Alborán Domain is under

* Corresponding author.
E-mail address: jabaloy@ugr.es (A. Jabaloy-Sánchez).

https://doi.org/10.1016/j.lithos.2018.07.026
0024-4937/

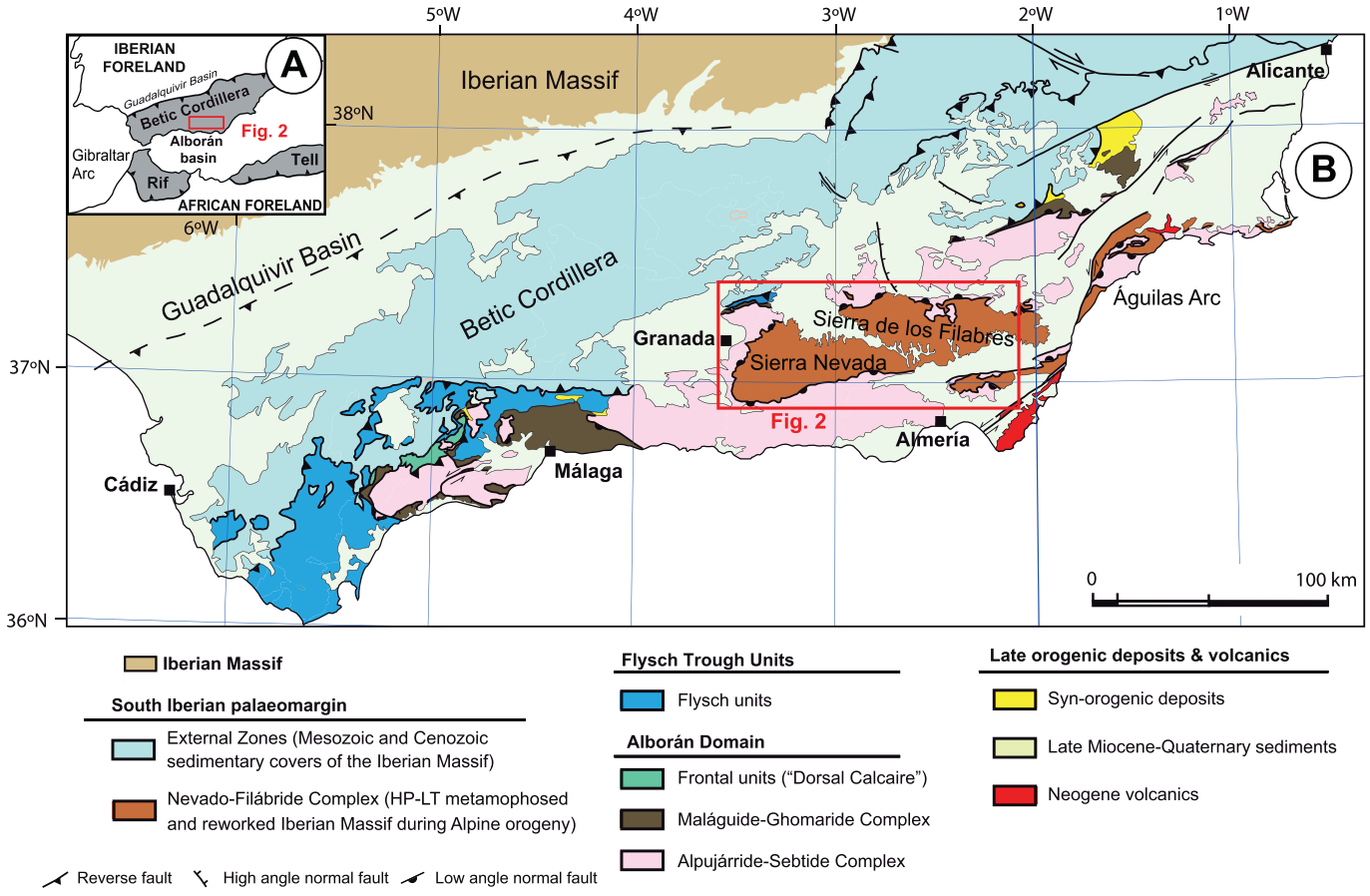

Fig. 1. A) Tectonic sketch of the Southwestern Mediterranean Sea, and B) Tectonic map of the Betic Cordillera.

discussion: one hypothesis locates these complexes in the microcontinent AlKaPeca (Bouillin et al., 1986), while an alternative hypothesis places these complexes near the South Iberian coast constituting an Alpine collisional chain (e.g. Platt et al., 2003).

Recently, Gómez-Pugnaire et al. (2012) proposed that the NFC can be related to the Central Iberian Zone of the Iberian Massif using U–Pb SHRIMP dating of magmatic zircons that yielded ages between ~282 ± 5 and 295 ± 3 Ma (Early Permian: Sakmarian to Artinskian). The Early Permian radiometric ages were determined on acid gneisses with associated metasomatic skarns, enclosed within metasedimentary sequences. Thus, a Paleozoic age was assigned to the sedimentary succession and their correlation with the granitoids of the Central Iberian Zone was proposed. In contrast, Rodriguez-Cañero et al. (2018) recently proposed that the NFC is related to the Cantabrian Zone of the Iberian Massif, deduced from the first conodont fauna described in this complex. Therefore, at present the paleogeographic domain for the NFC has not been definitively determined.

Distribution patterns of detrital zircon ages could help to constrain the age of formation of protoliths, and identify the source area of source allochthonous terrains. Studies on detrital zircons are scarce in the Betic Cordillera. They are limited to the Alpujárride and Maláguide complexes, yielding two probability density age plots (Esteban et al., 2017). For the NFC, Santamaría-López and Sanz De Galdeano (2018) proposed a Paleozoic age.

A broader suite of detrital zircon ages for these metasediments would provide independent maximum ages and might reveal the paleogeographical provenance of the Nevado-Filábride lithological successions. Accordingly, this work presents 891 SHRIMP and LA-ICPMS U–Pb zircon ages from 9 samples of metasedimentary quartzites selected from representative outcrops.

2. Geological setting

Five samples (SN-31b, SN-33, SN-36, SN-37 and SN-38) from Carboniferous psammites and metapsammites of the Aulago Fm outcropping in the western Sierra de los Filabres (Figs. 3 and 4, Table 1) were selected, with sample SN-31b located within the Río Boudurria unit, and the other four samples located within the Filabres unit. The four samples from the supposedly Permo-Triassic Tahal Fm were collected in the eastern Sierra de los Filabres (SN-47, SN-48, SN-49 and SN-51) (Fig. 5, Table 1).

The Betic Cordillera (Fig. 1) is the northern branch of the Betic-Rif orogenic belt, an Alpine arcuate mountain belt connecting the continental crusts of the southern Iberian Peninsula and the north-western African plate. This orogenic belt resulted from the collision of the allochthonous Alborán Domain with the southern paleomargin of the Iberian plate and the northern paleomargin of the African plate during the Neogene (i.e. Balanyá and García-Dueñas, 1987; Platt et al., 2013). During these collisions, the South Iberian Domain (Balanyá and García-Dueñas, 1987), was deformed by thin-skinned thrust-and-fold systems (e.g. 1; Platt et al., 2003; Meijninger and Vissers, 2007). The NFC is now considered one fragment of the southern palaeomargin of the Iberian massif that was subducted below the Alborán Domain and accreted below after undergoing Alpine HP-LT metamorphism and ductile deformations (see Gómez-Pugnaire et al., 2012; Booth-Rea et al., 2007, 2015; Behr and Platt, 2012; Platt et al., 2013, Jabaloy et al., 2015; Kirchner et al., 2016). Some authors maintain, however, that the Alborán Domain was essentially built during the Paleocene-Latest Oligocene (Azañón et al., 1997; Balanyá et al., 1997), in one N-directed subduction zone (e.g. Behr and Platt, 2012; Booth-Rea et al., 2007, 2015; Faccenna et al., 2004; Platt et al., 2013) as part of a continental terrane: the so-called "Alkapeca" terrane from Bouillin et al. (1986).

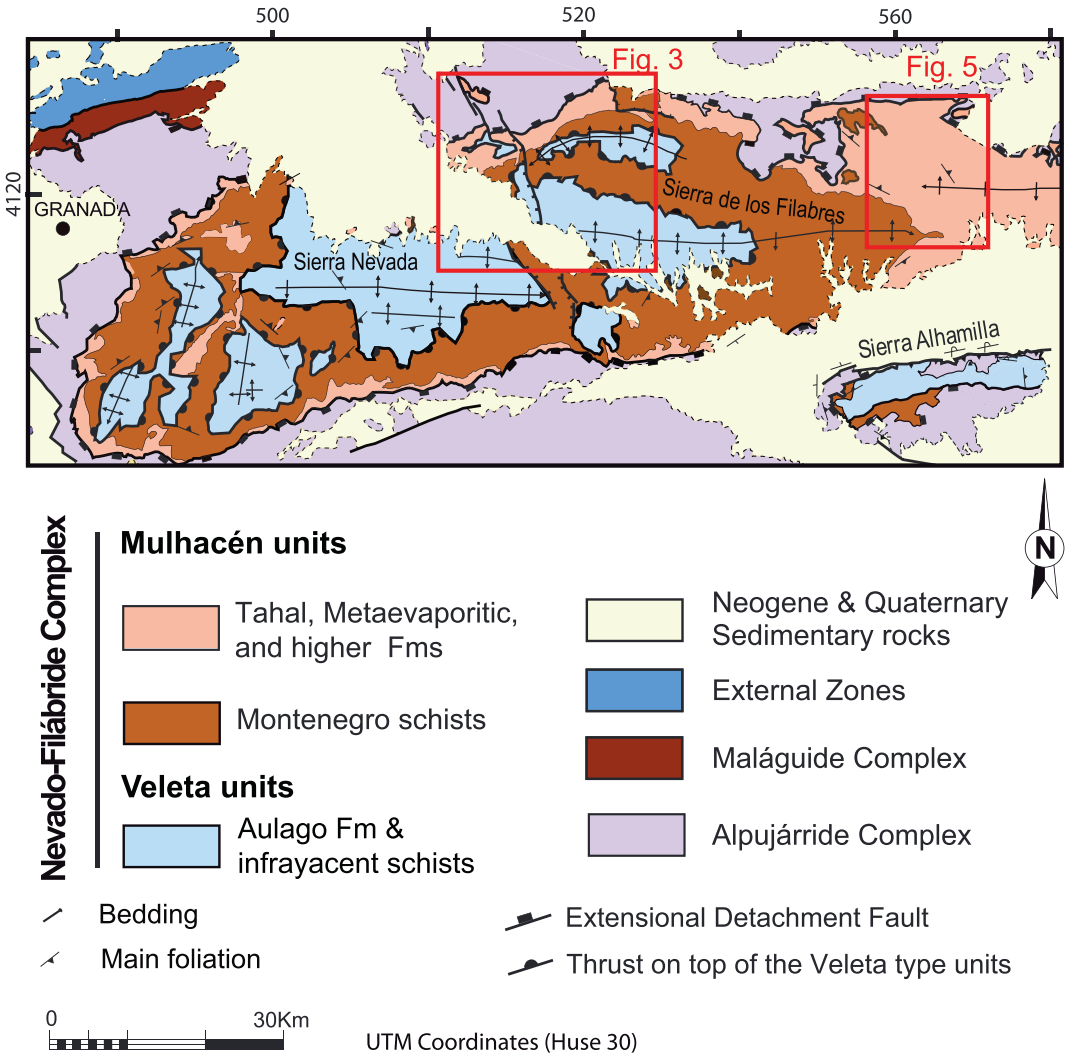

Fig. 2. Geological map of the southwestern Betic Cordillera with the main outcrop of the the Nevado-Filábride Complex (see Fig. 1 for location).

The NFC (Fig. 2) includes the Permo-Triassic Tahal Fm and the subjacent Paleozoic Veleta units containing the Carboniferous Aulago Fm, objects of our research. The NFC crops out in the central part of the Betic Cordillera, in the core of three mayor E-W trending antiforms (Sierra Alhamilla, Sierra Nevada, and Sierra de los Filabres; Fig. 2). Eastwards, left-handed strike-slip faults rotate and translate the folds towards the north to form the Águilas Arc (Fig. 1). Two major assemblages of tectonic units called Veleta (bottom) and Mulhacén (top) are commonly distinguished within the NFC in the Sierra Nevada (Fig. 2) (Martínez-Martínez, 1986; Puga et al., 1974). The original definition of these complexes (Puga et al., 1974) is not unanimously accepted at present in terms of name, number, tectonic units, or tectonic limits (i.e. Jabaloy et al., 2015; Platt et al., 2013; Santamaría-López and Sanz De Galdeano, 2018). However, given the common use of both terms in the NFC literature, it has been the custom to use both names for these sets of tectonic units instead of redefining them (see Figs. 1 to 5).

2.1. Lithological succession of the Veleta units

The lithological successions of the Veleta units in the Sierra Nevada and Sierra de los Filabres antiforms consist of low-grade metamorphic rocks from the Aulago Fm with alternating metapsamites with black phyllites superimposed on a monotonous and thick succession of low-grade black micaschists (Veleta schists, c.f. Puga et al., 1974, 2002; Gómez-Pugnaire, 1981; Martínez-Martínez, 1986) (Figs. 1, 2). Santamaría-López and Sanz De Galdeano (2018) dated detrital zircons from this succession and obtained a Carboniferous age (depositional ages younger than 349.1 ± 1.6 Ma, SHRIMP U–Pb).

In the Sierra de los Filabres antiform (Figs. 1, 2), the Veleta succession is duplicated into a little deformed lower Río Bodurria unit (Jabaloy, 1993; Rodriguez-Cañero et al., 2018), overlain by the strongly deformed upper Filabres unit (Figs. 3, 4). The Rio Bodurria unit is composed of white, fine-grained psammites and black slates from the Aulago Fm (Jabaloy, 1993; Martínez-Martínez, 1986) (Figs. 3 and 4) preserving sedimentary structures. At the base, 10 m of black limestones appear interlayered with black slates, which have provided Early Bashkirian conodont fauna (Rodriguez-Cañero et al., 2018). The colour alteration index (CAI index, Epstein et al., 1977) of the conodonts is 5 (Rodriguez-Cañero et al., 2018) corresponding to 300–480 °C (Epstein et al., 1977; Rejebian et al., 1987). The limestones are covered by ca. 250 m of alternating 1 to 10 m-thick packages of medium- to coarse-grained, whitish to greyish quartz-rich metapsammites (quartzwackes) formed of Qz + Ms + Bt + Pl + Chl ± Fsp. The metapsammites are separated by thin layers of black slates. The rocks preserve sedimentary structures, such as scour surfaces, graded bedding, parallel and cross-lamination, undulatory to lingoid ripples, flaser structures and burrows (Jabaloy, 1993; Rodriguez-Cañero et al., 2018).

The Filabres unit comprises low-grade black micaschists with microfossils indicating Neoproterozoic ages (Gómez-Pugnaire et al., 1982),

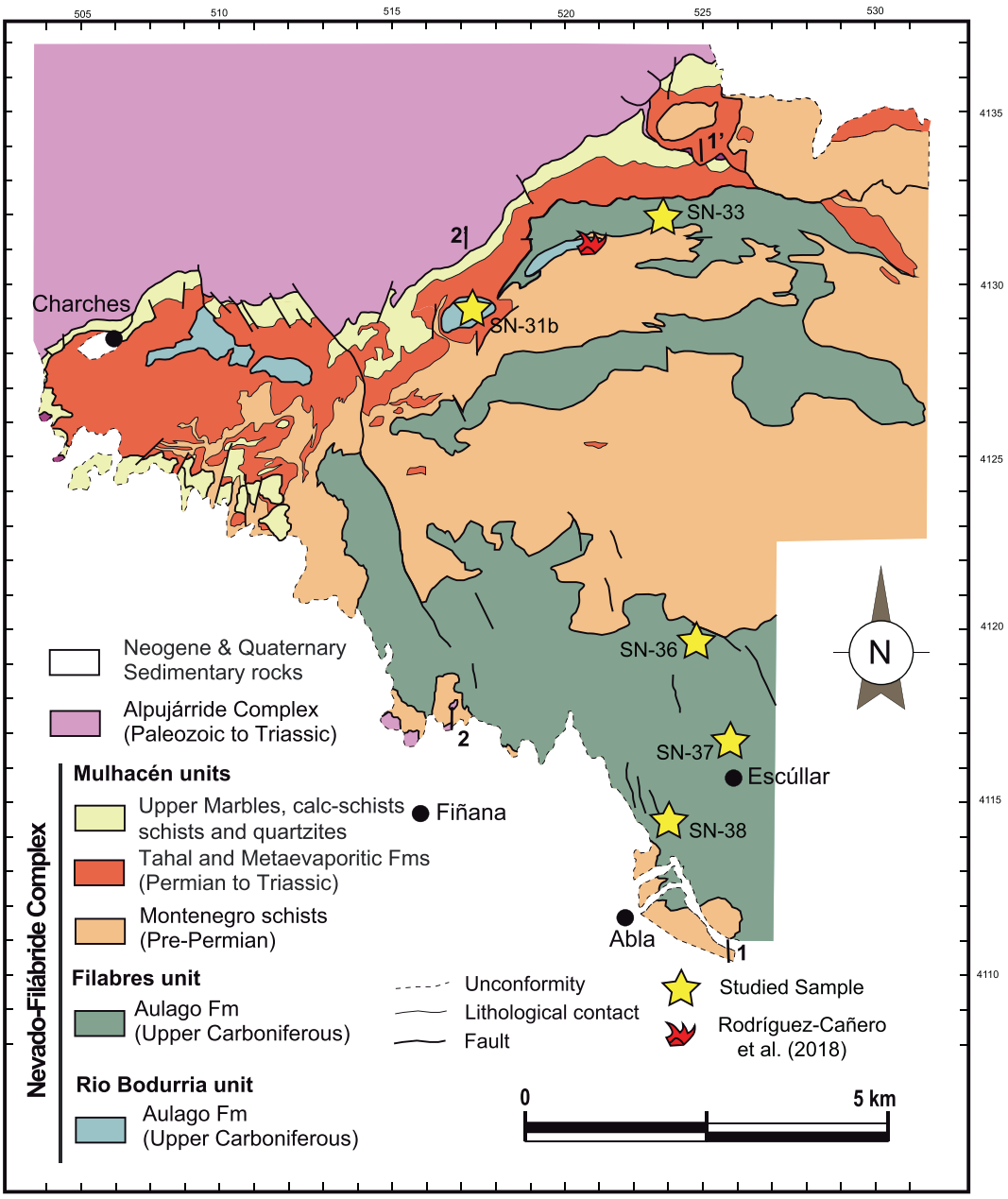

Fig. 3. Geological map of the western Sierra de los Filabres area (modified from Jabaloy, 1993; see Fig. 2 for location) with the location of the studied samples and of the conodont fauna described by Rodriguez-Cañero et al. (2018).

covered by 800 to 1200 m of metapsammites alternating with black phyllites and slates of the Aulago Fm. The metapsammites are whitish and cream rocks made up of Qz + Ms + Pl + Chl + Grt ± Bt, which crop out in 1.40 m-thick layers intercalated with black schists and phyllites. Although strongly deformed, they preserve parallel and cross-laminations marked by thin layers rich in zircon and rutile.

This Filabres unit reached peak temperatures of 350–480 °C during greenschists facies metamorphism (Gómez-Pugnaire and Franz, 1988), although Raman thermometry on graphite suggests higher temperatures (510–530 °C; Augier et al., 2005; Behr and Platt, 2012). Peak pressure during this metamorphic event is unclear as published values vary from 2 kbar (Gómez-Pugnaire and Franz, 1988) to 12–14 kbar (Booth-Rea et al., 2003).

In the Aguilas Arc (Fig. 1), the Veleta units (i.e. the Lomo de Bas unit) contain older successions that begin with graphite mica schists and phyllites which are overlaid by 80–140 m of thick, dark low-grade marbles (Álvarez-Lobato and Aldaya, 1985; Laborda-López et al., 2015a, 2015b), where abundant fossils indicate an Early-Middle Devonian age (Eifelian-Emsian, c.f. Lafuste and Pavillon, 1976; Laborda-López et al., 2013, 2015a, 2015b). This Devonian succession is overlain by a 130–500 m sequence of thick, very dark graphitic schist and phyllite, with intercalations of quartzite (Laborda-López et al., 2015a,b).

2.2. Lithological succession of the Mulhacén units

The Mulhacén units include a basal sequence of metasediments which underwent Alpine HP metamorphism at ca. 18–15 Ma (Gómez-Pugnaire et al., 2004, 2012; Platt et al., 2006) and are thrust over by a tectonic unit of ultramafic rocks (Jabaloy et al., 2015).

In the selected area, in the eastern of Sierra de los Filabres, the lithological succession consists of ca. 800 m of black micaschists dated as Upper Carboniferous by U–Pb SHRIMP (Montenegro Schists; Martínez-Martínez, 1986; Santamaría-López and Sanz De Galdeano,

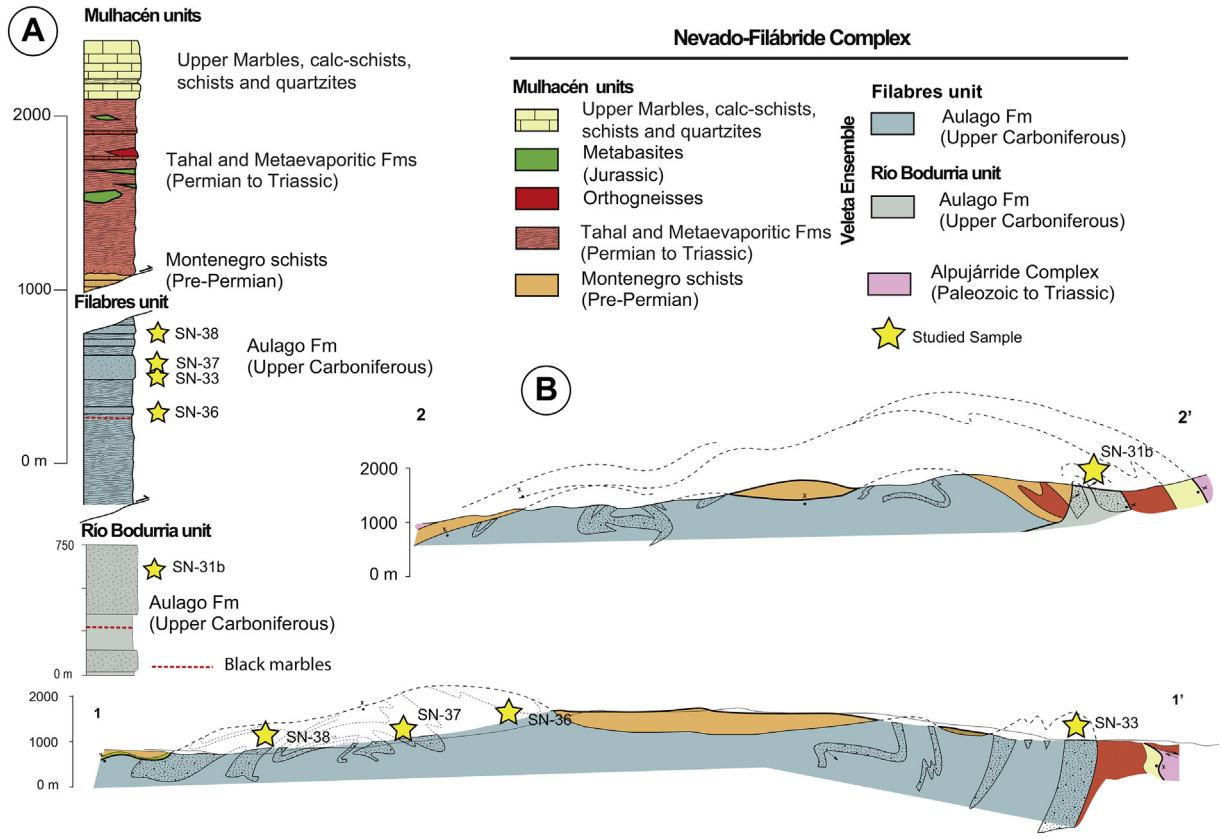

Fig. 4. A) Lithological columns of the Nevado-Filábride rocks, and B) geological cross sections of the western Sierra de los Filabres (modified from Jabaloy, 1993; see Fig. 3 for locations).

2018). These are overlain by a ca. 700 m of schists, metasandstones, and metaconglomerates of Permian age (Santamaría-López and Sanz De Galdeano, 2018) (Fig. 5) called the Tahal Fm (Voet, 1967), which is one of the lithologies sampled in this study. The Tahal Fm contains a lower ca. 400 m-thick sequence of metapsammites alternating with whitish and grey schists, preserving cross laminations and discontinuous layers of conglomerates (Vissers, 1981). The metapsammites are formed of Qz + Pl + Ms + Grt + Chl + Zrn. They are overlaid by an ca. 300 m of light grey schists.

The Tahal Fm is overlain by the Metaevaporite Fm (Gómez-Pugnaire et al., 1994) (Fig. 5), a thin (up to 80 m, usually <20 m) discontinuous succession of scapolite-gypsum-bearing marbles and fine-grained scapolite-gypsum-anhydrite-barite-bearing metapelites (Metaevaporitic Fm; Gómez-Pugnaire et al., 1994) that is covered by a ca. 700 m succession of micaschists, quartzites, marble and calc-schists (see López Sánchez-Vizcaino et al., 1997; Voet, 1967) (Fig. 5).

Metaultramafic rocks, interpreted as sub-continental lithosphere exhumed in a continental margin, thrust over the basal metasedimentary unit (Trommsdorff et al., 1998) and comprise antigorite-serpentinites derived from lherzolitic compositions that record prograde metamorphism during Middle Miocene subduction of the complex (c.f. Padrón-Navarta et al., 2011).

3. Analytical methods

Zircon grains were separated using standard heavy-liquid and magnetic techniques in the Department of Geodynamics of the University of Granada.

3.1. SHRIMP IIe/mc method

U-Th-Pb geochronological analyses were carried out on the SHRIMP IIe/mc instrument of the IBERSIMS lab, University of Granada. Hand-picked zircons from the studied samples, several grains of zircon reference standard TEMORA-II (for isotope ratios; Black et al., 2003), one grain of reference standard SL13 zircon (for U concentration, Claoue-Long et al., 1995), plus a few grains of REG zircon (high common lead,

Table 1
Location and lithology of the studied samples.

Sample	UTM zone	X	Y	Lithology	Succession	Methodology	Laboratory
SN31bis	30N	515,584	4,127,922	Sandstone within black schists	Aulago Fm (Río Bodurria Unit)	SHRIMP	University of Granada
SN-33	30N	520,306	4,130,073	Sandstone within black schists	Aulago Fm (Filabres unit)	SHRIMP	University of Granada
SN-36	30N	522,680	4,118,992	Sandstone within black schists	Aulago Fm (Filabres unit)	SHRIMP	University of Granada
SN-37	30N	523,932	4,116,119	Sandstone within black schists	Aulago Fm (Filabres unit)	SHRIMP	University of Granada
SN-38	30N	521,503	4,113,436	Sandstone within black schists	Aulago Fm (Filabres unit)	SHRIMP	University of Granada
SN-47	30N	560,668	4,118,706	Sandstone within white schists	Tahal Fm (Basal Mulhacén unit)	LA-ICP-MS	John de Laeter Center (JdLC), Curtin University, Perth
SN-48	30N	562,623	4,120,437	Sandstone within white schists	Tahal Fm (Basal Mulhacén unit)	LA-ICP-MS	John de Laeter Center (JdLC), Curtin University, Perth
SN-49	30N	562,789	4,122,373	Sandstone within white schists	Tahal Fm (Basal Mulhacén unit)	LA-ICP-MS	John de Laeter Center (JdLC), Curtin University, Perth
SN-51	30N	571,067	4,119,912	Sandstone within white schists	Tahal Fm (Basal Mulhacén unit)	LA-ICP-MS	John de Laeter Center (JdLC), Curtin University, Perth

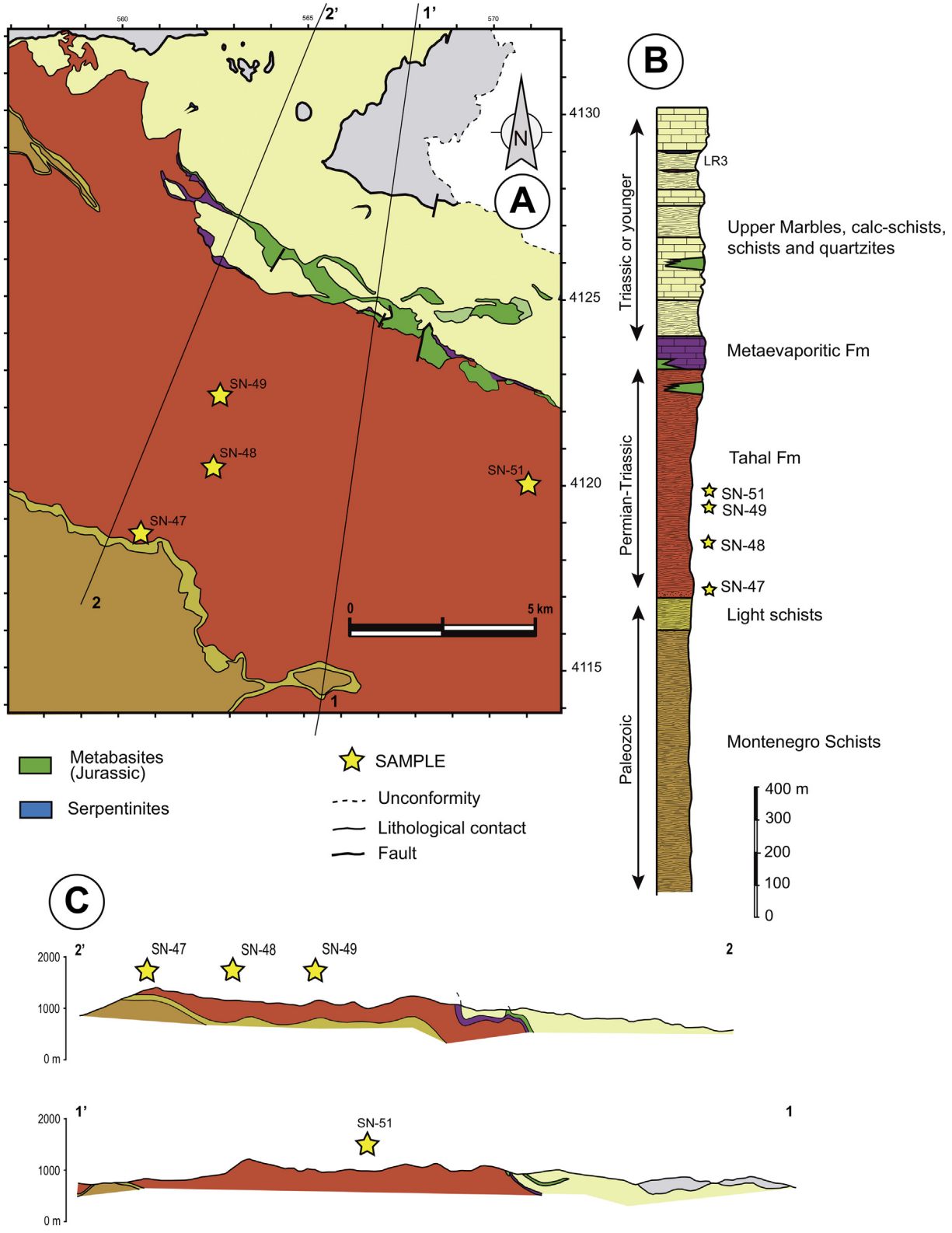

Fig. 5. A) Geological map of the eastern Sierra de los Filabres area (modified from García Monzón et al., 1973; see Fig. 2 for location). B) Lithological columns of the Nevado-Filábride rocks in the eastern Sierra de los Filabres. C) Geological cross sections of the eastern Sierra de los Filabres (modified from García Monzón et al., 1973).

for mass calibration) were mounted in a 3.5 cm diameter epoxy mount, polished and examined using optical (reflected and transmitted light) and scanning electron microscopy methods (secondary electrons (SE) and cathodoluminescence (CL)). After extensive cleaning, mounts were coated with ultra-pure gold (8–10 nm) and loaded for SHRIMP analysis.

The analytical method followed that described by Williams and Claesson (1987).

For zircons from metasedimentary samples, each selected spot was rastered with the primary beam for 90 s prior to analysis, and then analysed 4 scans, following the isotope peak sequence $^{196}Zr_2O$, ^{204}Pb, $^{204.1}$background, ^{206}Pb, ^{207}Pb, ^{208}Pb, ^{238}U, ^{248}ThO and ^{254}UO. Every

peak of every scan was measured sequentially 10 times with the following total counting times per scan: 2 s for mass 196; 5 s for masses 238, 248, and 254; 10 s for masses 204, 206, and 208; and 15 s for mass 207.

The primary beam, composed of $^{16}O^{16}O^{+}$, was set to an intensity of about 5 nA, with a 120 μm Kohler aperture that generated 17 × 20 μm elliptical spots on the target. The secondary beam exit slit was fixed at 80 μm, achieving a resolution of about 5000 at 1% peak height.

All calibration procedures were performed on the standards included on the same mount. A more detailed description of this method is included within the Supplementary material.

3.2. LA-ICPMS methods

LA-ICPMS data collection was performed at the GeoHistory Facility, John de Laeter Center (JdLC), Curtin University, Perth, Australia. Individual zircon grains (mounted and polished in 1″ epoxy rounds) were ablated using a Resonetics RESOlution M-50A-LR, incorporating a Compex 102 excimer laser, coupled to an Agilent 7700s quadrupole ICP-MS. Following a 30 s period of background analysis and two cleaning pulses, samples were spot ablated for 30 s at a 7 Hz repetition rate using a 33 μm beam and laser energy of 2.5 J/cm^2. The sample cell was flushed with ultrahigh purity He (350 mL min^{-1}) and N_2 (3.8 mL min^{-1}) and high purity Ar was employed as the plasma carrier gas (flow rate 0.98 L min^{-1}). For this work, the following elements were monitored for 0.03 s each: ^{28}Si, ^{29}Si, ^{49}Ti, ^{91}Sr, ^{147}Sm, ^{202}Hg, ^{204}Pb, ^{206}Pb, ^{207}Pb, ^{208}Pb, ^{232}Th, and ^{238}U. International glass standard NIST 610 was used as the primary standard to calculate elemental concentrations (using ^{29}Si as the internal standard element and assuming 14.76% Si in zircon) and to correct for instrument drift.

The primary age reference material used in this study was Plesovice (337.13 ± 0.37 Ma; Sláma et al., 2008) with 91,500 (1062.4 ± 0.4 Ma; Wiedenbeck et al., 1995), B188 (559 ± 8; Nasdala et al., 2004) and M257 (561.3 ± 0.3 Ma; Nasdala et al., 2008) used as secondary age standards. ^{206}Pb/^{238}U ages calculated for all zircon age standards, treated as unknowns, were found to be within 3% of the accepted value. The time-resolved mass spectra were reduced using the U_Pb_Geochronology4 data reduction scheme in Iolite3.5 (Paton et al., 2011, and references therein).

Errors cited for individual analysis are at the 2σ level. Dates where the concordant values were >110% or <90% were considered to be excessively discordant and were not considered in the age discussion or plotted on the Wetherill Concordia diagrams. However, they are listed on Tables 1S and 2S in the Supplementary material. Weighted mean values for ages given on pooled analyses are at the 95% confidence level.

4. Results

As two lithological units comprise the focus of this work, we group the results accordingly, differentiating between zircons from the Paleozoic (Carboniferous) lithologies: i.e. Aulago Fm, and those from the Permo-Triassic Tahal lithologies. Many measured zircons show similar internal structures (Figs. 6 and 7) that allow them to be classified into characteristic groups, as discussed below.

Some zircon crystals show an outer, thin, CL-dark, U-rich rim with either weak or no zoning (see SN-38Z 37 in Fig. 6 and SN-47z22 in Fig. 7). Similar rims have been also described in the orthogneisses from the Nevado-Filábride rocks and yield Miocene rim ages (Gómez-Pugnaire et al., 2004, 2012). They are interpreted as metamorphic rims formed during the HP-LT Metamorphic event (Gómez-Pugnaire et al., 2004, 2012) and were not targeted for U–Pb dating in this work.

Zircon grains mainly show continuous oscillatory zoning (Figs. 6 and 7), although there are also zircons with sector-zoning and some composite zircons with partially resorbed inner cores overgrown by inner rims (i.e. SN-31B_10 in Fig. 6, and SN-51z143 in Fig. 7). The cores can be rounded or euhedral and have diverse zoning patterns in all samples (i.e. SN-31B_10, SN-33_6, or SN-36_1 in Fig. 6, and SN-47z66, SN-48_z60, or SN-51z143 in Fig. 7). These inner rims display either oscillatory or sector zoning (i.e. SN-33_6 or SN-36_1 in Fig. 6, and SN-47z66 or SN-49z 127 in Fig. 7). U–Pb dates from this work were measured in all sectors and consistently yielded ages older than Upper Triassic (Tables 1S and 2S of the Supplementary material).

Zircons grains from the Aulago Fm are small (50 × 50 to 50 × 100 μm, Fig. 7), with most having rounded or elliptical morphologies. From CL imaging, these zircons mostly display continuous oscillatory zoning or comprise composite grains with a partially resorbed core overgrown by a rim (i.e. SN-36_1, Fig. 6). There are also some grains with sector zoning, and in two samples (SN-36 and SN-38), a few small prismatic crystals were found (i.e. SN-38_12, Fig. 6).

The zircon concentrates from the Tahal Fm provide rounded to elliptical zircons 60 × 50 μm in size, and euhedral grains around 200 μm in length. The CL images show zircons with continuous oscillatory zoning or complex grains with a partially reabsorbed core overgrown by a thick rim (i.e. SN-47z66, Fig. 7). There are also a few zircons with sector zoning and others that are structureless (SN47z26 and SN-49z105, respectively, Fig. 7).

4.1. Samples from the Aulago Fm

The SHRIMP U–Pb zircon data from the Aulago Fm (SN-31b, SN-33, SN-36, SN-37, and SN-38) are given in Table 1S of the Supplementary material and are plotted on the Concordia (Fig. 1S in the Supplementary material) and probability density diagrams (Fig. 8). Description of individual samples is also given in the Supplementary material.

The five samples are quite similar in terms of their zircon age spectra (Fig. 8). The youngest ^{206}Pb/^{238}U zircon grains in the individual samples range from 325 ± 6 Ma (SN-38) to 523 ± 6 Ma (SN-33). In the individual samples, the youngest zircon populations have ^{206}Pb/^{238}U ages between 562 ± 9 Ma (MSWD = 1.17 and probability = .32, SN-38) and 614 ± 10 Ma (MSWD = 0.63 and probability = .59, SN-31b) (Fig. 9).

Combined, the 342 SHRIMP U–Pb concordant-nearly concordant data from the Aulago Fm samples define a zircon age pattern composed of Paleozoic (9%), Neoproterozoic (51%), Mesoproterozoic (18%), Paleoproterozoic (12%), Neoarchean (8%), Mesoarchean (1%), Paleoarchean (~0.5%) and Eoarchean (~0.5%) dates (Fig. 8). On the age distribution plot, three main populations can be identified: Ediacaran, Cryogenian and Mesoproterozoic at ca. 596, 788 and 1031 Ma, respectively (Fig. 8). There are also three minor populations: two Paleoproterozoic (ca. 1.81 and 1.91 Ga) and one Neoarchean (ca. 2.62 Ga) (Fig. 8). Furthermore, these data yield one younger zircon population that consists of four analyses and has a ^{206}Pb/^{238}U age of 359 ± 5 (MSWD = 1.07, probability = .36) (Fig. 9).

4.2. Samples from the Tahal Fm

The zircon concentrates from the four metapsammite samples from eastern Sierra de los Filabres (see Fig. 5 for location) provide rounded to elliptical zircons 60 × 50 μm in size, and euhedral grains around 200 μm in length.

Information about the four samples are given in the Supplementary material (Table 2S, Fig. 2S) and in Fig. 10. These four samples display similar zircon age spectra (see Fig. 10). The youngest ^{206}Pb/^{238}U zircon age from the individual samples is 223 ± 5 Ma (SN-49), while the youngest zircon populations have ^{206}Pb/^{238}U ages between 274 ± 3 Ma (MSWD = 0.88 and probability = .45; SN-49) and 295 ± 3 Ma (MSWD = 1.4 and probability = .20; SN-47) (Fig. 11).

The zircon age pattern resulting from the 549 concordant-nearly concordant analyses from the Tahal Fm samples is composed of Mesozoic (<0.5%), Paleozoic (30%), Neoproterozoic (38%), Mesoproterozoic (7%), Paleoproterozoic (16%), Neoarchean (6%), Mesoarchean (2%) and Paleoarchean (<0.5%) zircon grains (Fig. 10). On the probability

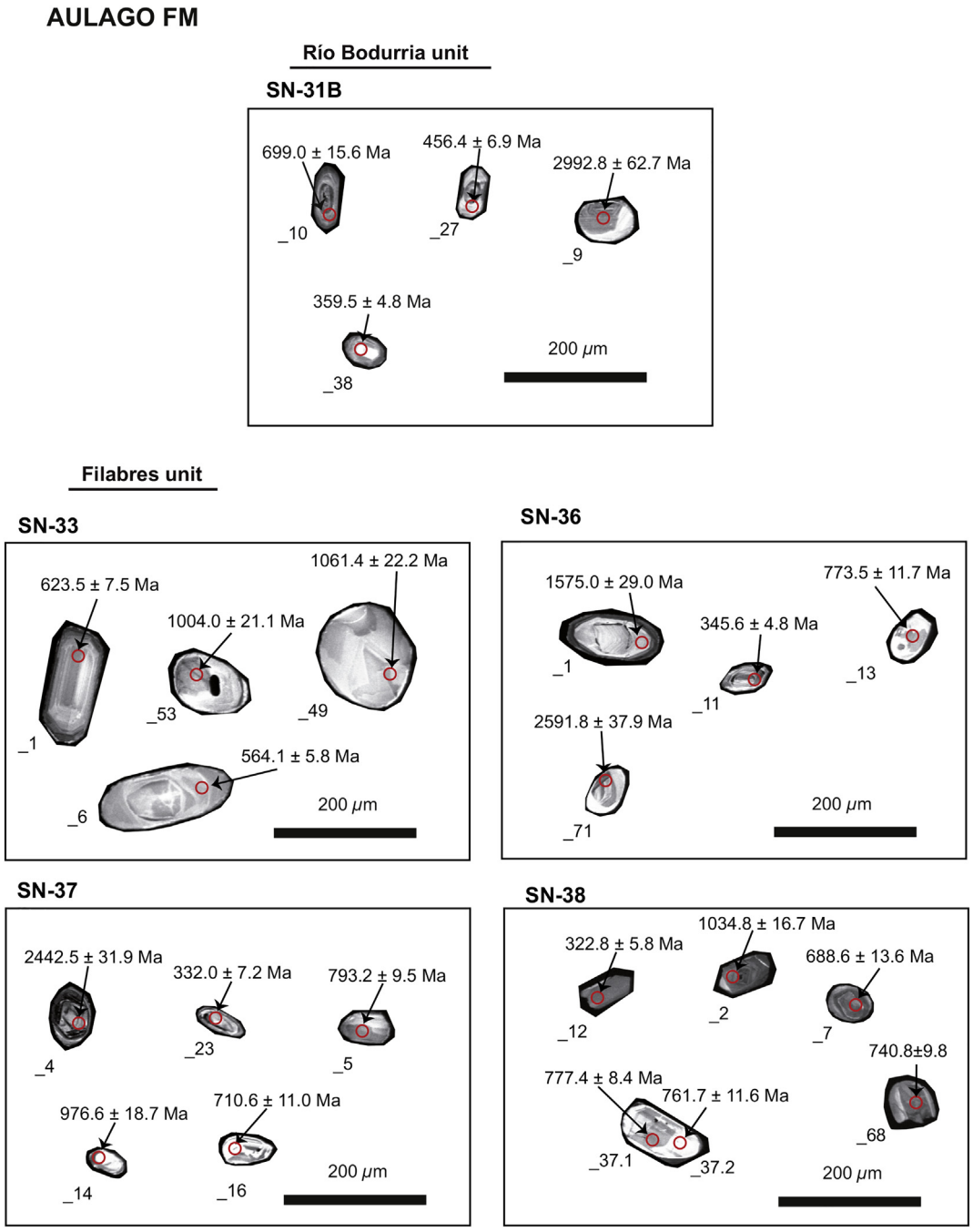

Fig. 6. Cathodoluminescence images of representative dated zircons of the samples from the Aulago Fm.

density plot, the dates cluster in five main populations: Permian (ca. 292 Ma), Ediacaran (ca. 594 Ma), Cryogenian (ca. 650 Ma), Tonian (ca. 992 Ma) and Mesoproterozoic (ca. 1052 Ma) (Fig. 10). Additionally, there are three minor populations: two Paleoproterozoic (ca. 1.88 and 1.96 Ga) and one Neoarchean (ca. 2.61 Ga) (Fig. 10). Furthermore, the youngest zircon population from the Tahal Fm is composed of 8 analyses and yields a $^{206}Pb/^{238}U$ mean age of 275 ± 2 Ma (MSWD = 1.10 and probability = .36) (Fig. 11).

5. Significance of the detrital zircon populations

5.1. Inherited detrital ages vs metamorphic ages

The calculated metamorphic peak temperatures are below the closure temperature of Pb, U and Th in zircon (~900 °C; Mezger and Krogstad, 1997): 300–480 °C in the Río Bodurria unit (Rodriguez-Cañero et al., 2018); 510 to 530 °C in the Veleta units (Augier et al., 2005), and 560 to 700 °C in the Mulhacén units (Gómez-Pugnaire et al., 1994; Jabaloy et al., 2015, and references therein).

Furthermore, the Th/U ratios show higher values than 0.01 (99% of the concordant-nearly concordant analyses, Tables 1S and 2S of the Supplementary material), similar to the Th/U ratio characteristic of magmatic zircons (Kirkland et al., 2015; Möller et al., 2003; Rubatto and Gebauer, 2000). Nevertheless, there are five zircons with low Th/U ratios, probably metamorphic in origin, but they yield older ages than those estimated for Alpine metamorphism. There are two grains from the Aulago Fm (SN31B-39.1 and SN36-73.1, Table 1S in Supplementary material) with Th/U ratios ≤0.01 that yield ca. 549 and 1034 Ma dates, respectively, while in the Tahal Fm, the three grains with Th/U < 0.01 (SN47z30, SN47z60r and SN47z133r, Table 2S in Supplementary

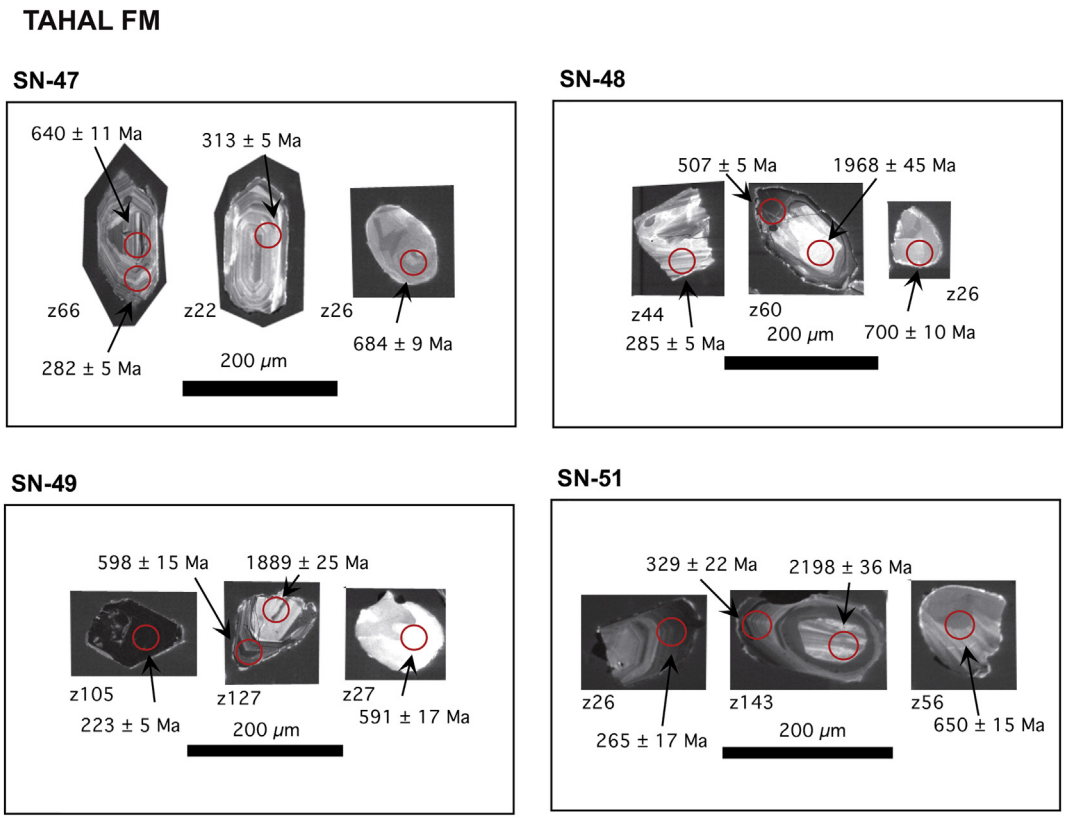

Fig. 7. Cathodoluminescence images of representative dated zircons from the Tahal Fm.

material) yield ages of ca. 406, 642 and 592 Ma, respectively. These data suggest a magmatic origin for more of 99% of the dated zircons.

6. Samples from the Aulago Fm

On the basis of our 342 concordant-nearly concordant data from the Aulago Fm, the maximum depositional age (defined by the $^{206}Pb/^{238}U$ date of the youngest zircon grain) is 325 ± 6 Ma (SN38-12.1, Table 2). A more conservative estimate of the maximum depositional age is given by the youngest zircon population that consists of four analyses and yields a $^{206}Pb/^{238}U$ age of 359 ± 5 Ma (MSWD = 1.07, probability = .36) (Fig. 9), pointing to an Upper Devonian-Lower Carboniferous maximum depositional age for the Aulago Fm metapsammites. The conodont fauna (Rodriguez-Cañero et al., 2018) found at the bottom of the Aulago Fm sets a Lowermost Bashkirian stratigraphic age for deposition of the first level of psammites. There is a ca. 35 Ma difference between the age of the faunal relics and the youngest zircon age population, thus, an Early Pennsylvanian age could be suggested as a plausible depositional age for the Aulago Fm. U–Pb SHRIMP detrital zircon ages from the dark schists in both the Veleta and the Mulhacén units (Santamaría-López and Sanz De Galdeano, 2018) identify a youngest zircon population at 349.1 ± 1.6 Ma, suggesting a Carboniferous age for the entire Veleta units and also the Montenegro schists within the Mulhacén units.

Rodriguez-Cañero et al. (2018) describe the Early Bashkirian conodont fauna in the black limestones interlayered with black slates at the base of the Aulago Fm and indicate that it is the same fauna present in the Barcaliente Fm (Wagner et al., 1971) of the Cantabrian Zone, northern Spain. The Barcaliente Fm is formed of black laminated limestones with high organic matter content (González Lastra, 1978), which are replaced upwards by siliciclastic sediments (Eichmüller and Seibert, 1984; González Lastra, 1978; Hemleben and Reuther, 1980), like those of the siliciclastic turbiditic deposits of the Olleros Fm, and the lower part of the Prioro Group (Rodríguez-Fernández, 1994). Furthermore, a very similar fauna was also found in the Iraty Fm from the western Pyrenees, which is overlaid by >800 m of shales, greywackes, and conglomerates of the Olazar Fm (de Boer et al., 1974, also known as Culm Facies unit). A similar Early to Late Bashkirian age is considered for siliciclastic deposits above the Iraty Fm in the western end of the Pyrenean Axial zone (see Sanz-López and Blanco Ferrera, 2012).

On the other hand, towards the Minorca, Catalonian Massif, Eastern Pyrenees, Mouthoumet Massif, and Montagne Noir Massif (see Martínez et al., 2016, and references therein), there are very different Upper Carboniferous successions compared to those in the Aulago Fm. A <100 m thick lower lithostratigraphic unit crops out and is composed of black chert with phosphate nodules, nodular limestone, and dark-green and dark-purple shales with a Tournaisian–lowermost Viséan age (Colmenero et al., 2002; Delvolvé, 1996). These rocks are covered by several thousand meters of "Culm series", consisting of siliciclastic turbidites with conglomerate, sandstone, and shales (Colmenero et al., 2002). Conglomerates contain clasts of Silurian and Devonian limestones (Delvolvé and Schulze, 1996; Sanz-López et al., 2006), Tournaisian black chert, and crystalline rocks in basins near the south Montagne Noire, (see Martínez et al., 2016, and references therein).

7. Samples from the Tahal Fm

The zircon grains from the Tahal Fm samples yield a youngest population of Lower Permian $^{206}Pb/^{238}U$ age, ranging from 295 ± 3 Ma at the base of the formation to 274 ± 3 Ma at the upper levels (samples SN-47 and SN-49 respectively) (Fig. 11). The youngest zircon has an Upper Triassic $^{206}Pb/^{238}U$ date (223 ± 5 Ma). Nevertheless, as at the Aulago Fm, we prefer a more conservative estimate for the maximum depositional

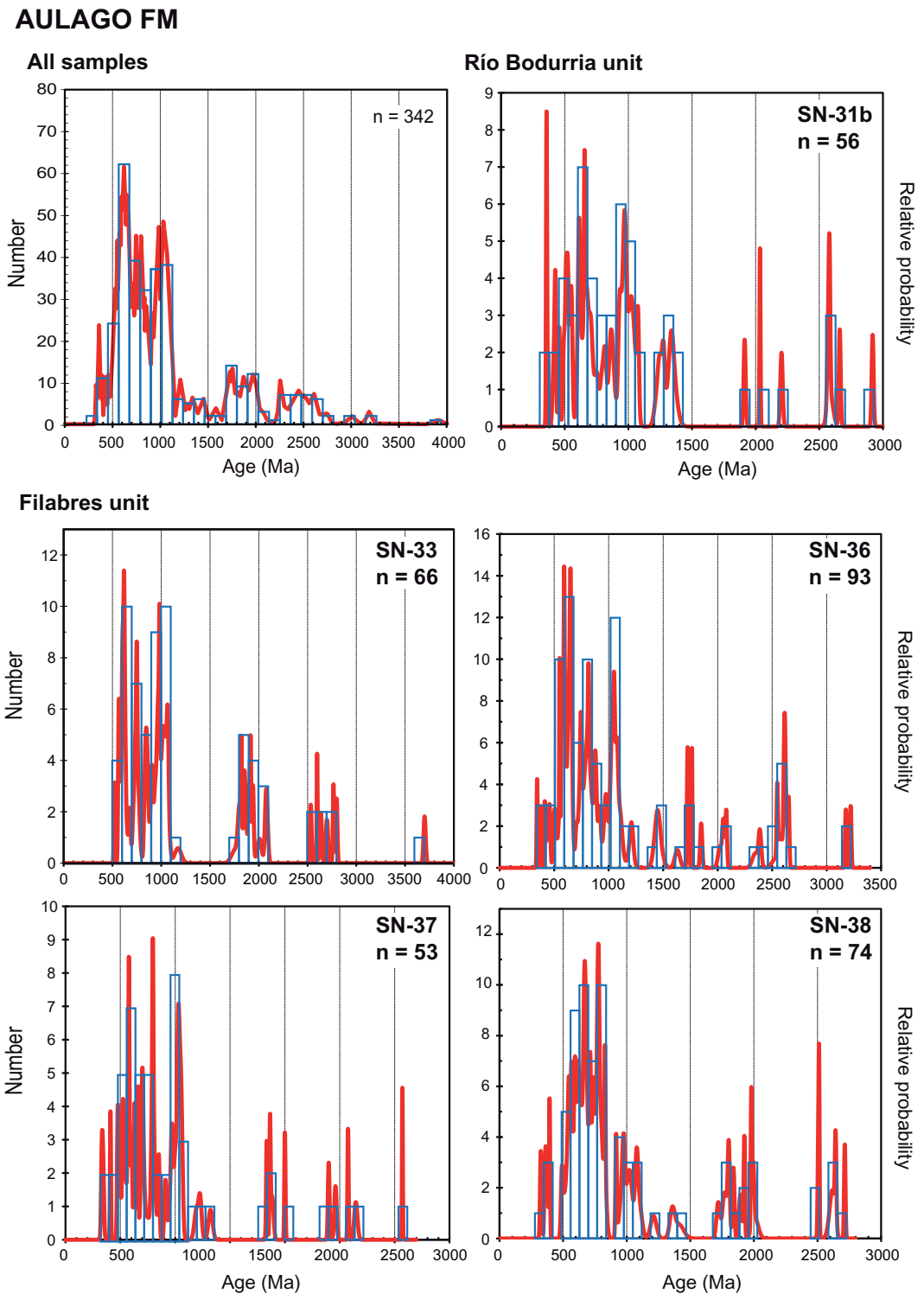

Fig. 8. U-Pb age probability plots for combined and individual samples from the Aulago Fm.

age of the Tahal Fm based on the youngest population, which indicates an age younger than the Early Permian (274 ± 3 Ma) age for the protoliths. Santamaría-López and Sanz De Galdeano (2018) studied 3 samples from the Tahal schists: 2 in Sierra Nevada (SF-2 and RA-3), and one in Sierra de los Filabres (VE-3, near our sample SN-47). They found youngest zircon populations ranging between 269.6 ± 0.9 Ma and 334.6 ± 2.9, which agrees with our data.

Similar successions overlaying unconformably the Variscan basement can be found in the Iberian Ranges, where a Middle Permian-Early Triassic sedimentary succession crops out and comprises two major sedimentary sequences of siliclastic red bed deposits with conglomerates, sandstones, siltstones, and clays, (see Sánchez Martínez et al., 2012 and references therein). Towards the Northeast, in the Eastern Pyrenees, there is an Upper Carboniferous to Permian succession composed of siliciclastic fluvio-lacustrine deposits, but with abundant volcanic bodies of calc-alkaline acidic to intermediate composition (Gretter et al., 2015, and references therein).

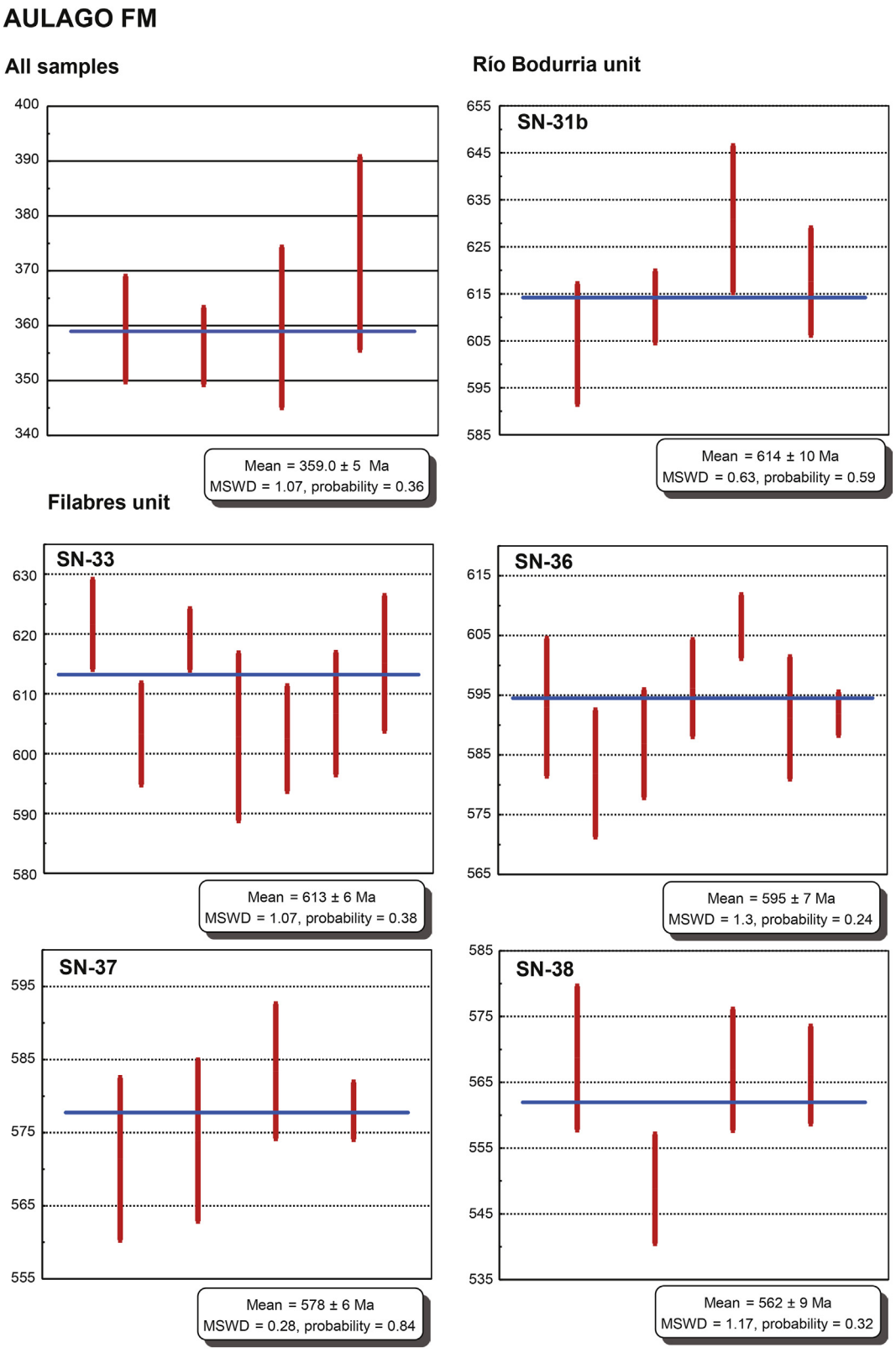

Fig. 9. Youngest zircon populations for combined and individual samples from the Aulago Fm.

Within the Maláguide Complex, the Triassic Saladilla Fm is composed of non-metamorphic continental redbeds (red mudstones, sandstones and conglomerates with some dolostone and gypsum beds; Roep, 1972), and shows Pseudoverrucano and Verrucano lithofacies (Perrone et al., 2006). These lie unconformably on the Marbella Conglomerate, which has been recently dated as Early Permian (Esteban et al., 2017), and is made up of a poorly sorted and polymictic conglomerate interlayered with a sandy sequence. It contains pebbles of quartzite, gneiss, granitoid, schist, aplite, dacite and other volcanic rocks.

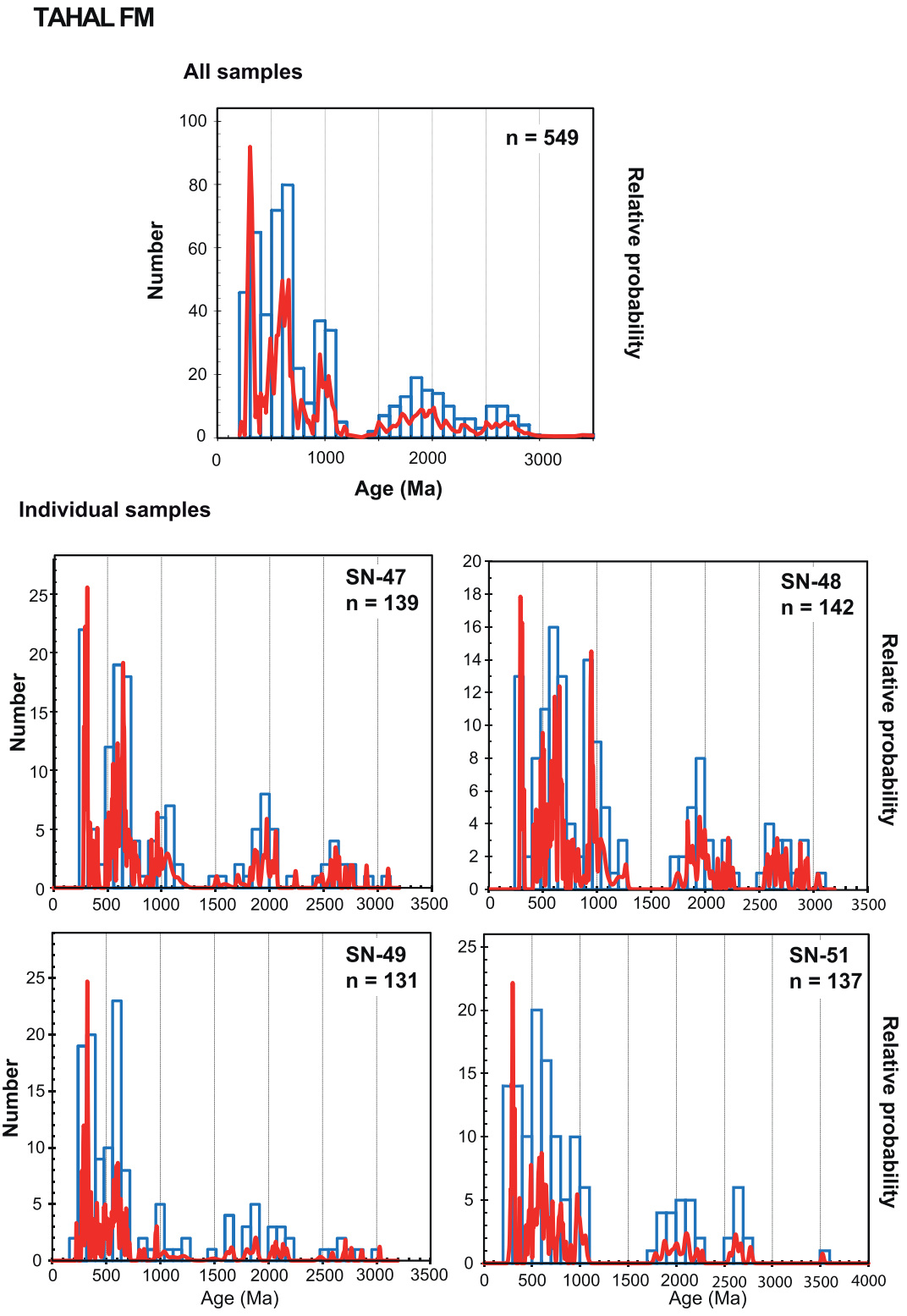

Fig. 10. U–Pb age probability plots for combined and individual samples from the Tahal Fm.

8. Paleogeographical implications

8.1. Comparison of the Aulago Fm with rocks from the West-Asturian Leonese and Cantabrian zones

To understand the position of the Aulago Fm during Late Carboniferous times, we compare the detrital zircon ages with datasets derived from zones with well-developed marine successions of the same age: i.e., the West-Asturian Leonese and Cantabrian zones (Cambeses, 2015; Cambeses et al., 2017; Martínez et al., 2016; Pastor-Galán et al., 2013), and the South Portuguese Zone (Cambeses, 2015; Cambeses et al., 2017; Pereira et al., 2012, 2014; Rodrigues et al., 2015) (Fig. 12). The Central Iberian, Galicia Tras-Os-Montes and Ossa Morena zones were not considered due to the absence of marine

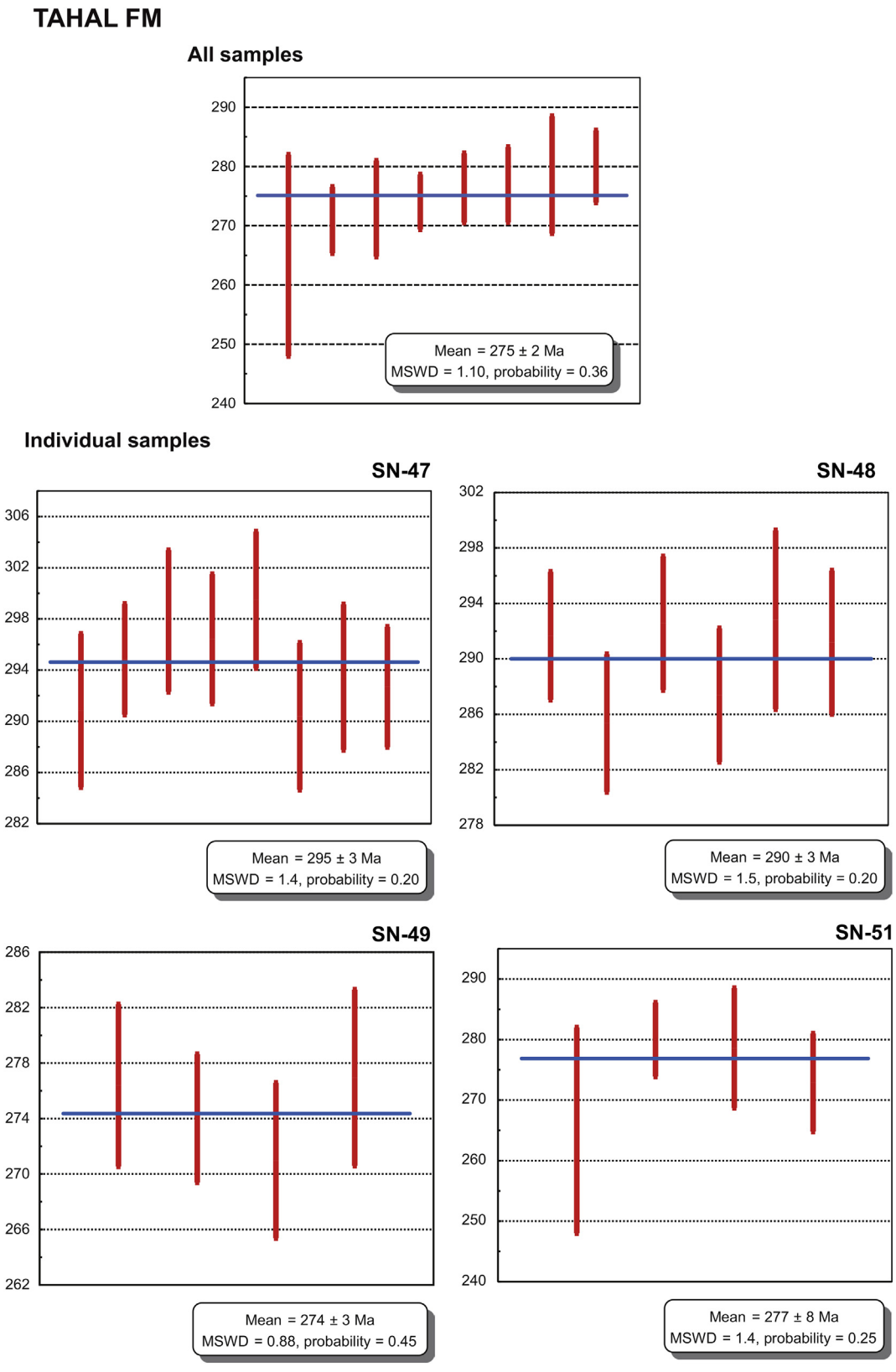

Fig. 11. Youngest zircon populations for combined and individual samples from the Tahal Fm.

Upper Carboniferous sediments in those areas at this time (i.e. Martínez Catalán, 2011, 2012).

Zircons in the Aulago Fm with Upper Ordovician, Silurian and Devonian ages (460 to 359 Ma) have no known source in the West-Asturian Leonese, and Cantabrian zones among other zones of the Iberian Massif. The nearest source of these zircon grains could be in the Avalonian terranes. During rifting and development of the Rheic Ocean between Avalonia and Gondwana, as well as during the later collision of Avalonian with Laurentia and Baltica (e.g. Sánchez Martínez et al., 2012, 2007), acidic magmatism developed that could be the source of

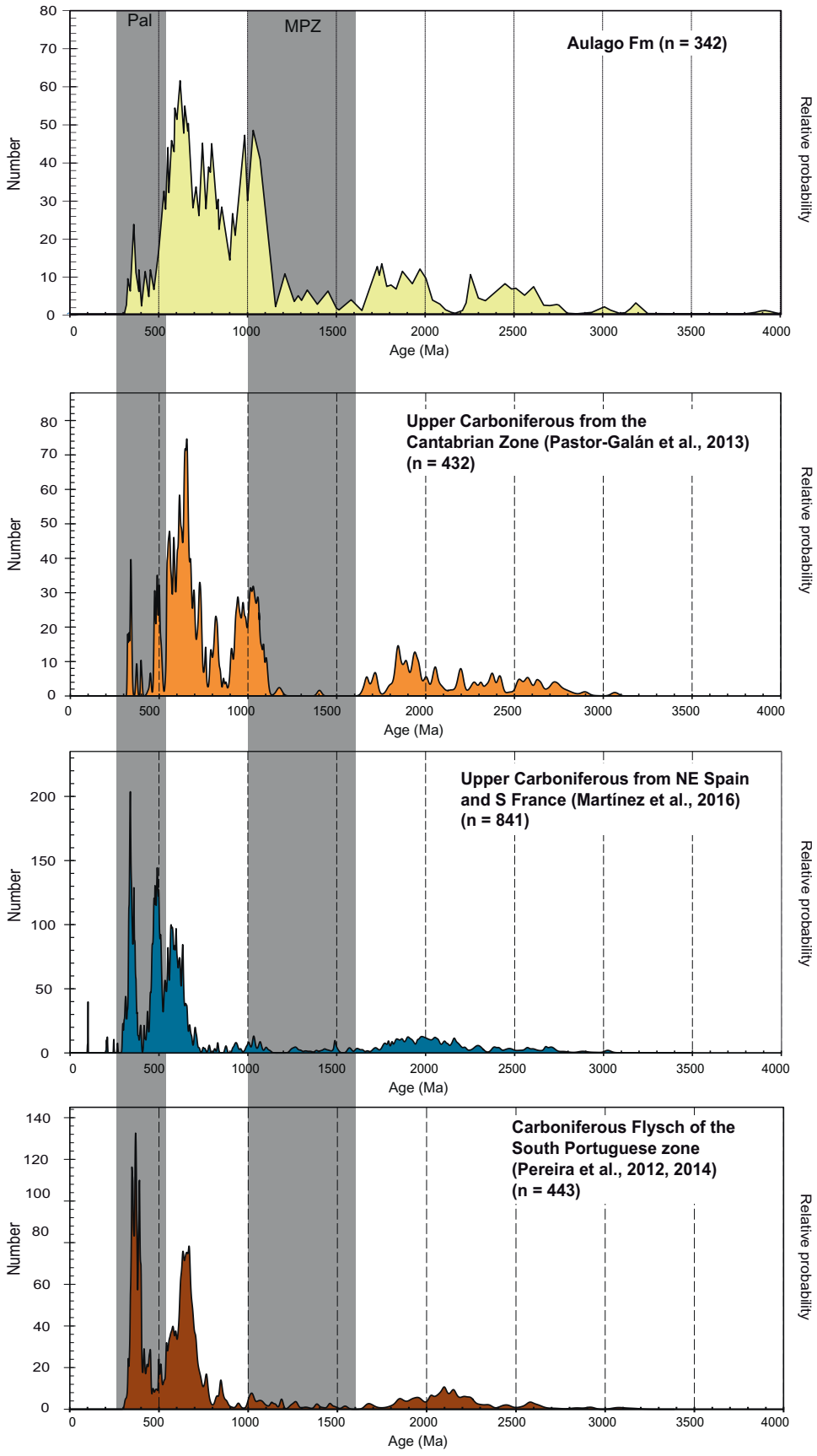

Fig. 12. Comparison between the U–Pb age probability plots from the Aulago Fm with those from other Upper Carboniferous rocks from the Cantabrian Zone, NE Spain and S France, and the South Portuguese Zone. Pal: Paleozoic, MPZ: Mesoproterozoic.

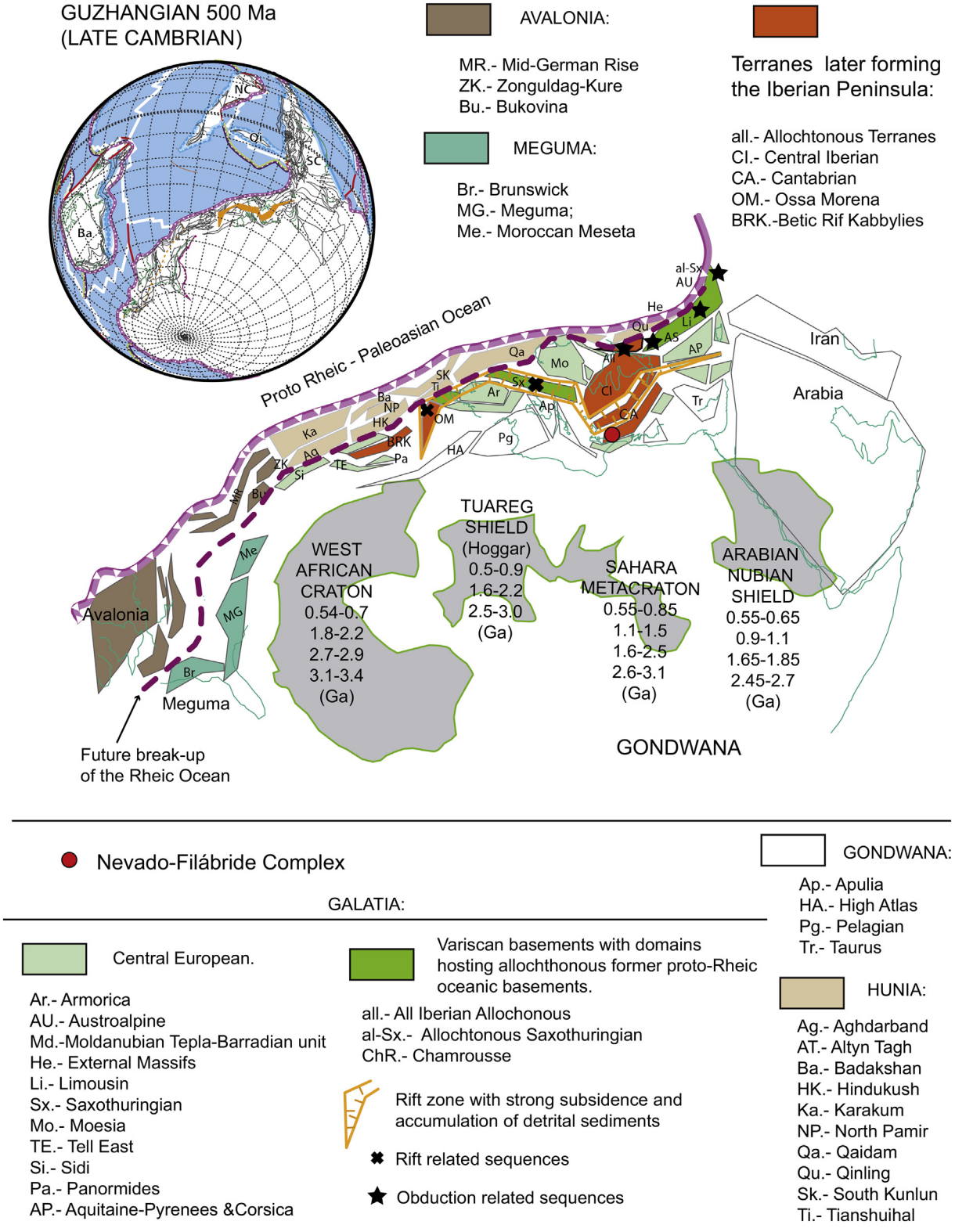

Fig. 13. Cambrian (500 Ma) plate-tectonic reconstruction modified after von Raumer et al. (2015) to include the main zircon populations in Africa and Arabia (after Abati et al., 2010 and Cambeses et al., 2017). The Location of the Nevado-Filábride complex at the end of the Cantabrian Zone is marked by a red dot.

the 460–359 Ma Aulago Fm zircons. In the syn-orogenic Lower and Middle Pennsylvanian sedimentary rocks of the Cantabrian Zone, zircons of similar ages to those found in the Aulago Fm. (Upper Ordovician, Silurian and Devonian) have also been interpreted as having been derived from the rocks of the Rheic Ocean suture zone (i.e. Pastor-Galán et al., 2013) (Fig. 12).

The predominant Ediacaran and Cryogenian populations in the Aulago Fm (ca. 596 and 788 Ma) are equivalent to the 540–850 Ma population in the Cantabrian Zone (Pastor-Galán et al., 2013). These dominant populations are also present in the Neoproterozoic to Paleozoic sediments in different zones of the Iberian Massif, including the West Astur-Leonian and Cantabrian zones (see Cambeses, 2015), and also in

the Neoproterozoic sediments from the Anti-Atlas and the West African Craton (Gärtner et al., 2017). Thus, the Ediacaran and Cryogenian zircon populations can be correlated to the Cadomian and Pan-African/Brasiliano orogenic event, recorded in the northern periphery of the Gondwana supercontinent (Linnemann et al., 2007, 2008; Nance and Murphy, 1994). This allows us to identify the northern Gondwana terranes and suggests that the Aulago Fm, as well as the above-mentioned zones of the Iberian Massif, could be part of the northern Gondwana terranes, located north of Africa in Cambrian-Ordovician times in agreement with many authors, such as Stampfli et al. (2013) and von Raumer et al. (2015) (see Figs. 13, 14 and 15).

The Tonian-Late Estenian population at ca. 1031 Ma was also found in the Carboniferous rocks in the Iberian Massif (but not in the South Portuguese Zone) (Bea et al., 2010; Cambeses, 2015; Cambeses et al.,

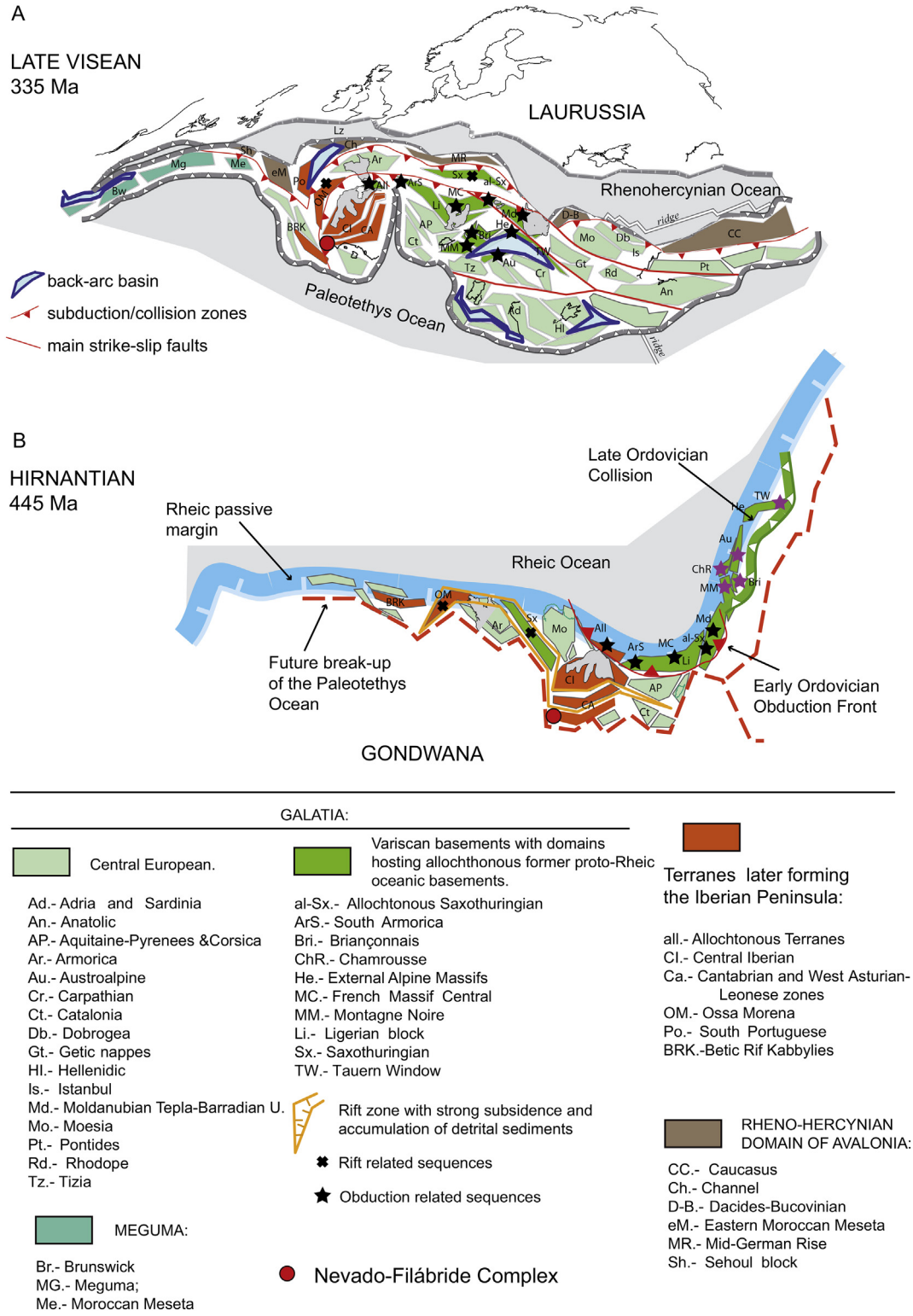

Fig. 14. Late Variscan (A) and Hirnantian (B) plate-tectonic reconstructions, modified after von Raumer et al. (2015), with the location of the Nevado-Filábride Complex marked by a red dot.

2017; Pastor-Galán et al., 2013, among others) (Fig. 12). The position of the Aulago Fm and also the Central Iberian, West Astur-Leonian and Cantabrian zones within the northern Gondwana terranes during the earliest Paleozoic is puzzling because basement rocks with these ages are not usually exposed in the North African areas (see Avigad et al., 2012; Bea et al., 2010). There is a characteristic lack of both Tonian and Late Estenian zircon in the West African Craton (Fig. 13), except in the far south (Volta Basin and Dahomeyides, Gärtner et al., 2017, and references therein). Furthermore, there are scarce amounts of Tonian zircons (6.7% of zircons, ranging from ~750 Ma to ~980 Ma) within the Lower Paleozoic sediments covering the Tuareg Shield (Linnemann et al., 2011) (Fig. 13). Also, Early Tonian (0.95 Ga) zircon U–Pb ages were obtained by Fezaa et al. (2010) on a coble embedded within Late Neoproterozoic metasediments in the eastern Hoggar. However, similar Tonian-Late Estenian populations have been described from Carboniferous rocks from the Sahara Metacraton (Meinhold et al., 2011) (Fig. 13). Also, Late Estenian zircon ages have been reported from sources within the East African Orogen and Israel (e.g. Bea et al., 2010; Avigad et al., 2012, and references therein), and from the Arabian-Nubian Shield (see Avigad et al., 2012; Bea et al., 2010 and references therein) (Fig. 13). Therefore, our Tonian-Late Estenian population can be explained, assuming that the nearest source for the Mesoproterozoic zircon population in the Aulago Fm was in the Sahara Metacraton, west of the Arabian-Nubian Shield (Fig. 13). Similar paleogeographic locations have been deduced for Ordovician samples from Sardinia (Meinhold et al., 2013) and eastern Pyrenees (Margalef et al., 2016). Furthermore, Bea et al. (2010) suggested that most of the Iberian massif zones were located east of the Saharan Metacraton in the Cambrian-Ordovician. Fig. 13 shows the possible location of the studied rocks within the plate tectonic reconstruction of the peri-Gondwanian basement terranes during Cambrian times (see Stampfli et al., 2013; von Raumer et al., 2015), previous to the scattering of those terranes by Variscan tectonic processes (Fig. 14). These tectonic processes included the opening of the Rheic Ocean (with an associated rift zone, strong subsidence and accumulation of detrital sediments), which caused the Avalonian and Hunian terranes to drift northwards (i.e. Stampfli et al., 2013; von Raumer and Stampfli, 2008) (see Figs 13 and 14). This was followed by the opening of the Paleotethys Ocean and the drifting of the Galatian terranes to collide with Laurussia during Carboniferous times (Fig. 14).

8.2. Comparison of the Aulago Fm with rocks of North-Eastern Spain and South France

Detritic zircon ages from the Carboniferous Flyschs of the Variscan outcrops in Minorca, Catalonian Massif, Eastern Pyrenees, Mouthoumet Massif, and Montagne Noir Massif were studied by Martínez et al. (2016) (Fig. 12). Those rocks were deposited during Late Visean to Middle Bashkirian times and show different detrital zircon population distributions to those of the Aulago Fm. The main difference is the absence of the Tonian-Late Estenian and the Cryogenian populations that are well represented in the Aulago Fm (Fig. 12). Furthermore, as there is a prominent Ediacaran age zircon population in our samples that is not strongly represented in the southern France and northeastern Spain zones (Fig. 12), the Aulago Fm cannot be correlated with the French and Spanish zones.

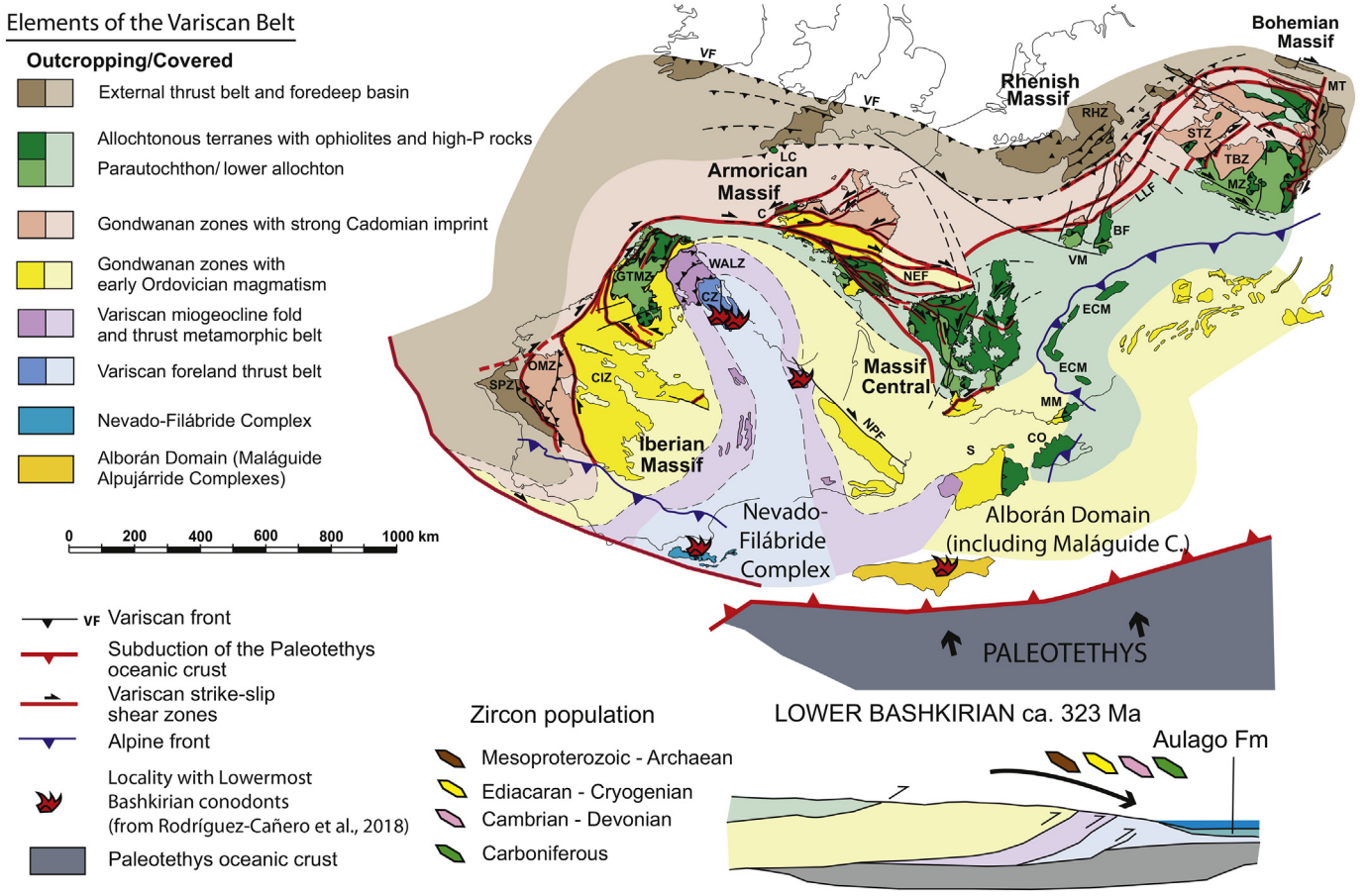

Fig. 15. Paleogeography of the eastern Variscan belt at Early Bashkirian times, during the deposition of the Aulago Fm. Modified from Rodríguez-Cañero et al. (2018) and Martínez Catalán (2011): CIZ, Central Iberian; CZ, Cantabrian; GTMZ, Galicia-Trás-os-Montes; MGCZ, Mid-German Crystalline; MZ, Moldanubian; OMZ, Ossa-Morena; RHZ, Rheno-Hercynian; SPZ, South Portuguese; STZ, Saxo-Thuringian; TBZ, Teplá-Barrandian; WALZ, West Asturian-Leonese.

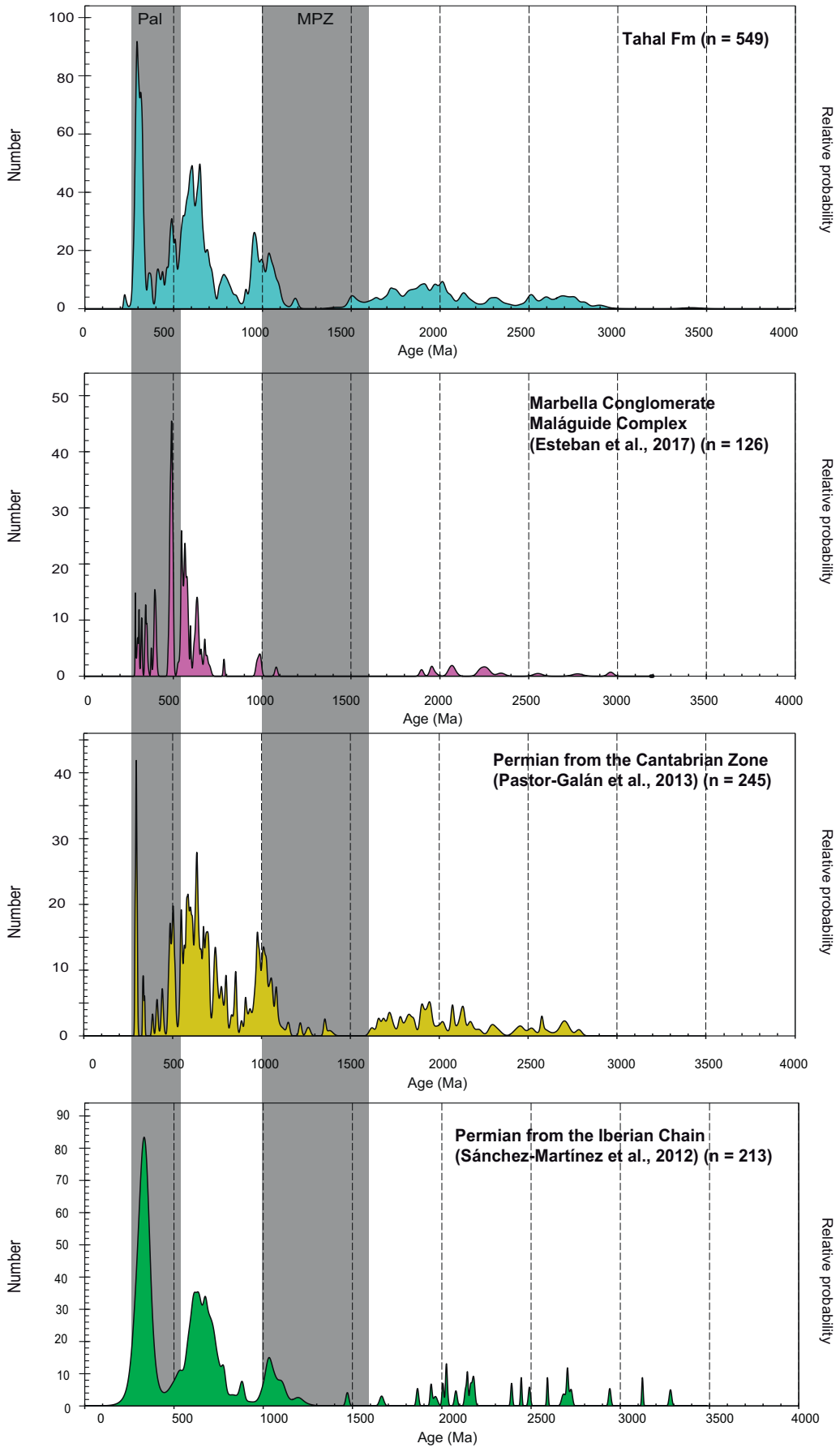

Fig. 16. Comparison between the U–Pb age probability plots for the Tahal Fm and for other Permian rocks from the Maláguide Complex, Cantabrian Zone, and the Iberian Chain. Pal: Paleozoic, MPZ: Mesoproterozoic.

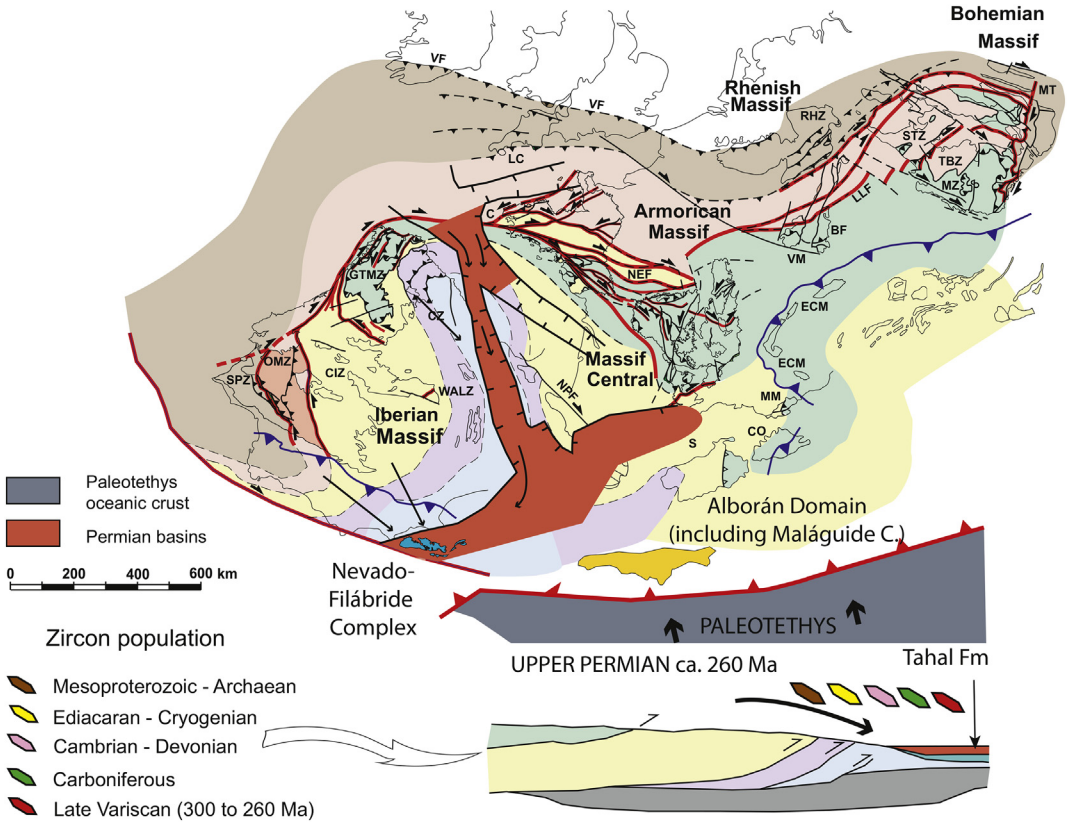

Fig. 17. Paleogeography of the eastern Variscan belt at Upper Permian times, during the deposition of the Tahal Fm. Modified from Rodriguez-Cañero et al. (2018) and Martínez Catalán (2011): CIZ, Central Iberian; CZ, Cantabrian; GTMZ, Galicia-Trás-os-Montes; MGCZ, Mid-German Crystalline; MZ, Moldanubian; OMZ, Ossa-Morena; RHZ, Rheno-Hercynian; SPZ, South Portuguese; STZ, Saxo-Thuringian; TBZ, Teplá-Barrandian; WALZ, West Asturian-Leonese. The Permian basins are modified from Sánchez Martínez et al. (2012).

8.3. Comparison of the Aulago Fm with with rocks from South Portuguese Zone

In the South Portuguese Zone, the Upper Carboniferous Baixo Alentejo Flysch Group comprises three formations from Late Visean to Late Moscovian (345–307 Ma; Pereira et al., 2012, 2014 and references therein). This Group is dominated by a Carboniferous population, and there is a secondary cluster within the 400–612 Ma age group. Additionally, detrital zircons with Mesoproterozoic ages (0.9–1.1 Ga) are not well represented (Pereira et al., 2012, 2014; Rodrigues et al., 2015) and this Group shows a very different population distribution pattern to the Aulago Fm detrital zircons. The South Portuguese Zone, together with the Rheno-Hercynian Zone, are considered to be external thrust belts and foredeep basins related to the Avalonian terranes (Frischmuth, 1968; Oliveira et al., 1979; von Raumer et al., 2017) (see Fig. 15).

In summary, the detrital zircon age data from the Aulago Fm and that from the Lower and Middle Pennsylvanian syn-orogenic successions in the Cantabrian Zone are similar (Figs. 12 and 15), but they have a very different age distribution pattern to rocks with similar ages from the South Portuguese Zone, southeastern France, and northeastern Spain.

8.3.1. Source rocks for the Tahal Fm

The Lower Permian zircon population may record erosion of the igneous rocks ascribed to the Late-Variscan magmatic event (ca. 300 to ca. 275 Ma, i.e. Vai et al., 1984; Cassinis et al., 2000; Gutiérrez-Alonso et al., 2011). This population may also record erosion of the alkaline igneous rocks generated during the transition from the Late-Variscan event to the Alpine cycle (Gretter et al., 2013; Stampfli and Kozur, 2006), which accounts for the scarcity of Lower-Middle Permian zircons (ca. 290–260 Ma).

The erosion and recycling of Variscan belt rocks can be identified by the presence of the Paleozoic to Neoarchean populations in the Tahal Fm. The older populations include the Upper Carboniferous (295 to 320 Ma), which corresponds to the early manifestations of the Late-Variscan magmatic event, and an Upper Ordovician population (480 Ma) related to magmatic events developed in the northern margin of Gondwana during the opening of the Rheic Ocean. Furthermore, there are Cryogenian (590 to 640 Ma), Tonian (950 to 990 Ma), Paleoproterozoic (1950 to 1970 Ma), and Neoarchean populations (2600 to 2615 Ma) that we have previously described in the rocks of the Aulago Fm and which point to source areas from the eroding Variscan Chain.

8.4. Comparison of Tahal Fm with other successions from the Iberian Peninsula

There is only one published U–Pb detrital age spectrum from the Maláguide Complex (Esteban et al., 2017) obtained in the Paleozoic Marbella Conglomerate. This limits opportunities for comparison between the Tahal zircon populations and the Alborán Domain. In the studied outcrop, Esteban et al. (2017) found an Early Permian youngest zircon at ca. 286 Ma, a zircon age distribution characterised by a lack of Mesoproterozoic ages (between 1700 and 1000 Ma) and scarce Middle to Early Neoproterozoic ages (950 to 750 Ma) (Fig. 16). The data from the Marbella Conglomerate are distinct from the zircon populations in the Tahal samples as the latter are characterised by one Mesoproterozoic (ca. 1052 Ma) main population (Fig. 16). Furthermore, the zircon age distribution for the Alpujárride Complex (compiled by Esteban et al., 2017), although slightly different to that of the Maláguide Complex, shows the same scarcity of Mesoproterozoic zircons.

On the contrary, Pastor-Galán et al. (2013) presented data for two Permian samples from the Cantabrian Zone and the distribution patterns are very similar to the samples from the Tahal Fm as they contained Proterozoic (850–540 Ma, 41%; 1150–900 Ma, 20% to 25%; 2150–1750 Ma, 11 to 20%; and 2800–2500 Ma, 2 to 7%), and Paleozoic populations (510–475 Ma, 2 to 10%; 360–320 Ma, 2 to 5%; 310–290 Ma, 1 to 10%) (Fig. 16). The latter Lower Permian population, however, is slightly older (310–290 Ma, the youngest zircon dates being at 298 and 290 Ma; Pastor-Galán et al., 2013) than the Tahal Fm (the youngest population at ca. 295 to ca. 274 Ma, and the youngest zircons at ca. 285 to ca. 223 Ma).

Sánchez Martínez et al. (2012) also studied several samples from the Permo-Triassic Series of the Iberian Ranges and found that the source areas of the sediments contain zircons with a range of ages. Samples from the Middle-Upper Permian and Middle Triassic rocks are distinguished by a dominant population of Variscan (290–360 Ma) zircons, important populations of Cadomian zircons (520–750 Ma), and the presence of Mesoproterozoic zircons, indicating a relationship with long fluvial systems eroding the core of the Ibero-Armorican arc (Fig. 16). However, the Lower Triassic sediments are characterised by scarce Variscan zircons (4% to 7%) and a higher proportion of Cadomian (38%–45%), Mesoproterozoic (17%–20%), Eburnian (10%–11%), and post-Eburnian and Archaean (8%–12%) populations (Sánchez Martínez et al., 2012). Sánchez Martínez et al. (2012) therefore proposed that the main source areas in this time period were located further away from the Variscan axial zone, probably into the Laurussia continent. Our data from the Tahal Fm are in agreement with the data from the Middle-Upper Permian and Middle Triassic rocks of the Iberian range (Fig. 17), indicating similar source areas, from the axial zone of the Variscan belt. This suggests prolongation of the Iberian Permian basins towards the NFC (Figs. 17 and 18), but there is no evidence to support a Laurussia continent provenance.

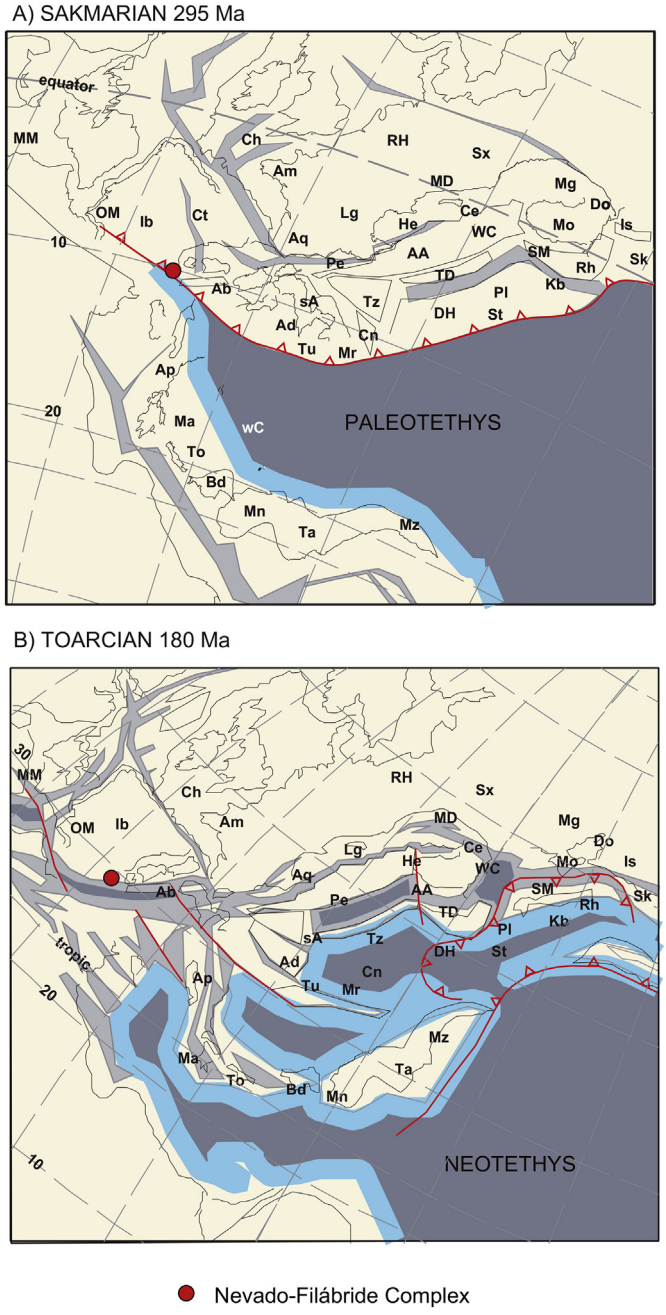

Fig. 18. Late Paleozoic (Sakmarian, A) and Early Jurassic (Toarcian, B) plate-tectonic reconstructions, modified after Stampfli and Kozur (2006), with the location of the Nevado-Filábride Complex marked by a red dot.

The zircon populations of the Aulago and Tahal Fms indicate a paleogeographic location for both formations within the Cantabrian Zone of the Iberian Massif, in agreement with the results obtained by Rodriguez-Cañero et al. (2018) using conodonts (Figs. 15 and 15). These populations also provide new evidence about the adscription of the NFC into the South Iberian Domain and also redefine the Alborán Domain as constituting only the Alpujárride and the Maláguide complexes (Gómez-Pugnaire et al., 2004, 2012; Platt et al., 2013). Our data suggest that the NFC rocks represent the parautochtonous Iberian Massif overthrust by the Alborán Domain, and therefore, they most likely moved together during the evolution of the Paleotethys and Neotethys oceans (see Figs. 13, 14, and 18).

9. Conclusions

Zircons from Nevado-Filábride Complex metamorphic rocks yielded 891 concordant-nearly concordant $^{206}Pb/^{238}U$ inherited detrital ages. The 342 concordant-nearly concordant data from the metapsammitic Aulago Fm indicate a Pennsylvanian age as the maximum depositional age for the Aulago Fm, in agreement with recently described conodont fauna in the same rocks (Rodriguez-Cañero et al., 2018). Comparison of the detrital zircon age spectra with the existing data from Upper Carboniferous rocks from Minorca, Catalonian Massif, Eastern Pyrenees, Mouthoumet Massif, Montagne Noir Massif, and South Portuguese Zone of the Iberian massif did not yield enough similarities to indicate that the Nevado-Filábride Complex rocks were deposited in paleogeographic areas similar to those mentioned. On the contrary, detrital zircons populations in the Aulago Fm indicate that the protolith of this formation was very similar to that of the Iberian Massif and specifically that of the Cantabrian Zone (North of the Iberian Massif). Furthermore, the main Ediacaran and Cryogenian populations, at ca. 596 and 788 Ma respectively, in the Aulago Fm relate the Nevado-Filábride Complex to the northern Gondwana terranes (Pastor-Galán et al., 2013), while the Mesoproterozoic population at ca. 1031 Ma (Tonian-Late Estenian population) suggests that it can be located north of the Saharan Metacraton and near the East African Orogen during the Cambrian-Ordovician, similar to the Central Iberian, West-Astur-Leonian and Cantabrian zones (Bea et al., 2010).

The 549 concordant-nearly concordant analyses from the Tahal Fm yield an Early Permian age for the protoliths. The detrital zircon age pattern records erosion of Late-Variscan and the erosion of alkaline igneous rocks testifying the transition from the Late Variscan to the Alpine cycle, accompanied by the recycling of rocks from the Variscan igneous and sedimentary rocks. Comparison with data from the Maláguide and Alpujárride complexes (Esteban et al., 2017) adds new evidence in support of considering the Nevado-Filábride Complex as part of the South Iberian Domain and supports the redefinition of the Alborán Domain as comprising the Alpujárride and Maláguide complexes

(Gómez-Pugnaire et al., 2004, 2012; Platt et al., 2013). The data from the Tahal Fm are similar to those from the Permo-Triassic rocks of the Iberian Ranges (Sánchez Martínez et al., 2012) suggesting extension of the Iberian Permian basins towards the NFC. The presented zircon ages from the Nevado-Filábride Complex record the erosion of Iberian Massif rocks during the late stages of the Variscan Orogeny (Late Carboniferous), and the beginning of the paleomargin stage during the Permian.

Acknowledgements

We thank Ricardo Arenas and Jürgen von Raumer for their constructive reviews of the submitted version of the manuscript. We also want to thank Antonio Azor for his helpful comments during the writing of the manuscript. We are indebted to B. McDonald for his technical support on the LA-ICPMS and Chris Kirkland for his insights into data reduction. The CL imaging was carried out on the Curtin University's JdLC Microscopy & Microanalysis Facility, whose instrumentation has been partially funded by the University, State and Commonwealth Governments. This work is supported by grants RNM-P12-3141 (Junta de Andalucía, Spain), CGL2016-75224-R, and CGL2015-71692-P (MINECO/FEDER, Spain), the Australian Research Council (LE150100013) and AuScope NCRIS (AQ44 Australian Education Investment Fund program).

Appendix A. Supplementary data

Supplementary data to this article can be found online at https://doi.org/10.1016/j.lithos.2018.07.026.

References

Abati, J., Aghzer, A.M., Gerdes, A., Ennih, N., 2010. Detrital zircon ages of Neoproterozoic sequences of the Moroccan Anti Atlas belt. Precambrian Research 181, 115–128.

Álvarez-Lobato, F., Aldaya, F., 1985. Las unidades de la Zona Bética en la región de Águilas-Mazarrón (Prov. de Murcia). Estudios Geológicos 41, 139–146.

Augier, R., Booth-Rea, G., Agard, P., Martínez-Martínez, J.M., Jolivet, L., Azañón, J.M., 2005. Exhumation constraints for the lower Nevado-Filabride complex (Betic Cordillera, SE Spain): a Raman thermometry and TWEEQU multiequilibrium thermobarometry approach. Bulletin de la Société Géologique de France 176, 419–432.

Avigad, D., Gerdes, A., Morag, N., Bechstädt, T., 2012. Coupled U-Pb-Hf of detrital zircons of Cambrian sandstones from Morocco and Sardinia: implications for provenance and Precambrian crustal evolution of North Africa. Gondwana Research 21, 690–703.

Azañón, J.M., Crespo-Blanc, A., García-Dueñas, V., 1997. Continental collision, crustal thinning and nappe forming during the pre-Miocene evolution if the Alpujarride Complex (Alboran Domain, Betics). Journal of Structural Geology 19, 1055–1077.

Balanyá, J.C., García-Dueñas, V., Azañón, J.M., Sánchez-Gómez, M., 1997. Alternating contractional and extensional events in the Alpujarride nappes of the Alborán domain (Betics, Gibraltar Arc). Tectonics 16, 226–238.

Balanyá, J.C., García-Dueñas, V., 1987. Les directions structurales dans le Domaine d'Alborán de part et d'autre du Détroit de Gibraltar. Comptes Rendus de l'Académie des Sciences de Paris 304, 929–932.

Bea, F., Montero, P., Talavera, C., Abu Anbar, M., Scarrow, J., Molina, J.F., Moreno, J.A., 2010. The palaeogeographic position of Central Iberia in Gondwana during the Ordovician: evidence from zircon geochronology and Nd isotopes. Terra Nova 22, 341–346.

Behr, W.M., Platt, J.P., 2012. Kinematic and thermal evolution during two-stage exhumation of a Mediterranean subduction complex. Tectonics 31, TC4025.

Black, L.P., Kamo, S.L., Allen, C.M., Aleinikoff, J.A., Davis, D.W., Korsch, J.R., Foudolis, C., 2003. TEMORA 1: a new zircon standard for Phanerozoic U-Pb geochronology. Chemical Geology 200, 155–170.

Booth-Rea, G., Martínez-Martínez, J.M., Giaconia, F., 2015. Continental subduction, intracrustal shortening, and coeval upper-crustal extension: PT evolution of subducted south Iberian paleomargin metapelites (Betics, SE Spain). Tectonophysics 663, 122–139.

Booth-Rea, G., Azañón, J.M., Goffé, B., Vidal, O., Martínez-Martínez, J.M., 2003. High-pressure, low-temperature metamorphism in Alpujarride units of southeastern Betics (Spain). Comptes Rendus de l'Académie des Sciences de Paris 334, 1–9.

Booth-Rea, G., Ranero, C.R., Martínez-Martínez, J.M., Grevemeyer, I., 2007. Crustal types and tertiary tectonic evolution of the Alborán Sea, western Mediterranean. Geochemistry, Geophysics, Geosystems 8 (10), Q10005.

Bouillin, J.P., Durand-Delga, M., Olivier, P., 1986. Betic-Rifian and Tyrrhenian arcs: distinctive features, genesis and development stages. In: Wezel, F.C. (Ed.), The Origin of Arcs. Elsevier Science, Amsterdam, pp. 281–304.

Cambeses, A., 2015. Ossa-Morena Zone Variscan 'Calc-Alkaline' Hybrid Rocks: Interaction of Mantle- and Crustal-Derived Magmas as a Result of Intra-Orogenic Extension Related Intraplating. Universidad de Granada, Ph.D. Thesis (450 pp).

Cambeses, A., Scarrow, J.H., Montero, P., Lázaro, C., Bea, F., 2017. Palaeogeography and crustal evolution of the Ossa–Morena Zone, southwest Iberia, and the North Gondwana margin during the Cambro-Ordovician: a review of isotopic evidence. International Geology Review 59, 94–130.

Cassinis, G., Di Stefano, P., Massari, F., Neri, C., Venturi, C., 2000. Permian of South Europe and its interregional correlation. In: Yin, H.F., Dickins, J.M., Shi, G.R., et al. (Eds.), Permian–Triassic Evolution of Tethys and Western Circum-Pacific. Elsevier Science, Amsterdam:pp. 37–70 https://doi.org/10.1016/S0920-5446(00)80005-9.

Claoue-Long, J.C., Compston, W., Roberts, J., Fanning, C.M., 1995. Two Carboniferous ages: a comparison of SHRIMP zircon dating with conventional zircon ages and $^{40}Ar/^{39}Ar$ analysis. In: Berggren, W.A., Kent, D.V., Aubry, M.P., Hardenbol, J. (Eds.), Geochronology Time Scales and Global Stratigraphic Correlation. SEPM (Society for Sedimentary Geology), pp. 3–21 Special Publication No. 4.

Colmenero, J.R., Fernández, L.P., Moreno, C., Bahamonde, J.R., Barba, P., Heredia, N., González, F., 2002. Carboniferous. In: Gibbons, W., Moreno, T. (Eds.), The Geology of Spain. Geological Society of London, London, pp. 93–116.

de Boer, H.U., Krausse, M.F., Mohr, K., Pilger, A., Requadt, H., 1974. La région de magnésite d'Eugui dans les Pyrénées Occidentales espagnoles: une explication de la carte géologique. Pirineos 111, 21–39.

Delvolvé, J.J., 1996. Carbonifère à facies Culm. In: Barnolas, A., Chiron, J.C. (Eds.), Synthèse Géologique et Géophysique des Pyrénées. Tome 1-Cycle Hercynien. Bureau de Recherches Géologiques et Minières-Instituto Tecnológico y Geominero de España, Orléans and Madrid, pp. 303–338.

Delvolvé, J.J., Schulze, H., 1996. Evolution des flyschs synorogéniques. In: Barnolas, A., Chiron, J.C. (Eds.), Synthèse Géologique et Géophysique des Pyrénées. Tome 1-Cycle Hercynien. Bureau de Recherches Géologiques et Minières-Instituto Tecnológico y Geominero de España, Orléans and Madrid, pp. 589–591.

Eichmüller, K., Seibert, P., 1984. Faciesentwicklumg zwischen Tournai und Westfal D mi.Kantabrischen Gebirge (NW-Spanien). Zeitschrift der Deutschen Geologischen Gesellschaft 135, 165–191.

Epstein, A.G., Epstein, J.B., Harris, L.D., 1977. Conodont color alteration-an index to organic metamorphism. Geological Survey Professional Paper 995, 1–27.

Esteban, J.J., Cuevas, J., Tubía, J.M., Gutiérrez-Alonso, G., Larionov, A., Sergeev, S., Hofmann, M., 2017. U–Pb detrital zircon ages from the Paleozoic Marbella Conglomerate of the Malaguide Complex (Betic Cordilleras, Spain): Implications on Paleotethyan evolution. Lithos 290-291, 34–47.

Faccenna, C., Piromallo, C., Crespo-Blanc, A., Jolivet, L., Rossetti, F., 2004. Lateral slab deformation and the origin of the western Mediterranean arcs. Tectonics 23. https://doi.org/10.1029/2002TC001488.

Fezaa, N., Liégeois, J.-P., Abdallah, N., Cherfouh, E.-H., De Waele, B., Bruguier, O., Ouabadi, A., 2010. Late Ediacaran geological evolution (575–555 Ma) of the Djanet Terrane, Eastern Hoggar, Algeria, evidence for a Murzukian intracontinental episode. Precambrian Research 180, 299–327.

Frischmuth, E., 1968. Sedimentation und Tektonik in der Subvariszischen Vortiefe von Süd—Portugal. Münstersche Forschungen zur Geologie und Paläontologie 4 (p. 99 p, Münster).

García Monzón, G., Kampschuur, W., Vissers, R., 1973. Mapa Geológico de España escala 1: 50,000 n° 1013 (Macael). Instituto Geológico y Minero de España (IGME), Madrid, Spain.

Gärtner, A., Youbi, N., Villeneuve, M., Sagawe, A., Hofmann, M., Mahmoudi, A., Boumehdi, M.A., Linnemann, U., 2017. The zircon evidence of temporally changing sediment transport-the NW Gondwana margin during Cambrian to Devonian time (Aoucert and Smara areas, Moroccan Sahara). International Journal of Earth Sciences 106 (8), 2747–2769.

Gómez-Pugnaire, M.T., 1981. Evolución del metamorfismo alpino en el Complejo Nevado-Filábride de la Sierra de Baza (Cordilleras Béticas, España). Tecniterrae 4, 1–130.

Gómez-Pugnaire, M.T., Chacón, J., Mitrofanov, V., Timofeev, V., 1982. First report on the Precambrian rocks in the graphite-bearing series of the Nevado-Filábride complex (Betic Cordilleras, Spain). Neues Jahrbuch für Geologie und Paläontologie, Monatshefte 3, 176–180.

Gómez-Pugnaire, M.T., Franz, G., 1988. Metamorphic evolution of the Paleozoic series of the Betic Cordilleras (Nevado-Filabride complex, SE Spain) and its relationship with the Alpine orogeny. Geologische Rundschau 77, 619–640.

Gómez-Pugnaire, M.T., Franz, G., López Sánchez-Vizcaíno, V., 1994. Retrograde formation of NaCl-scapolite in high pressure metaevaporites from the Cordilleras Béticas (Spain). Contributions to Mineralogy and Petrology 116, 448–461.

Gómez-Pugnaire, M.T., Galindo-Zaldívar, J., Rubatto, D., González-Lodeiro, F., López Sánchez-Vizcaíno, V., Jabaloy, A., 2004. A reinterpretation of the Nevado-Filábride and Alpujárride Complex (Betic Cordillera): field, petrography and U-Pb ages from orthogneisses western Sierra Nevada, S Spain. Schweizerische Mineralogische und Petrographische Mitteilungen 84, 303–322.

Gómez-Pugnaire, M.T., Rubatto, D., Fernández-Soler, J.M., Jabaloy, A., López Sánchez-Vizcaíno, V., González-Lodeiro, F., Galindo-Zaldívar, J., Padrón-Navarta, J.A., 2012. U–Pb geochronology of Nevado–Filábride gneisses: evidence for the Variscan nature of the deepest Betic complex (SE Spain). Lithos 146-147, 93–111.

González Lastra, J., 1978. Facies salinas en la Caliza de Montaña (Cordillera Cantábrica). Trabajos de Geología, Universidad de Oviedo 10, 249–265.

Gretter, N., Ronchi, A., López-Gómez, J., Arche, A., De la Horra, R., Barrenechea, J., Lagoe, M., 2015. The Late Palaeozoic-Early Mesozoic from the Catalan Pyrenees (Spain): 60 Myr of environmental evolution in the frame of the western peri-Tethyan palaeogeography. Earth-Science Reviews 150, 679–708.

Gretter, N., Ronchi, A., Langone, A., Perotti, C.R., 2013. The transition between the two major Permian tectono-stratigraphic cycles in the central Southern Alps: results from facies analysis and U/Pb geochronology. International Journal of Earth Sciences 102, 1181–1202.

Gutiérrez-Alonso, G., Fernández-Suárez, J., Jeffries, T.E., Johnston, S.T., Pastor-Galán, D., Murphy, J.B., González, M.P.F., Gonzalo, J.C., 2011. Diachronous post-orogenic magmatism within a developing orocline in Iberia, European Variscides. Tectonics 30, TC5008. https://doi.org/10.1029/2010TC002845.

Hemleben, C.H., Reuther, C.-D., 1980. Allodapic limestones of the Barcaliente Formation (Namurian A) between Luna and Cea Rivers (Southern Cantabrian Mountains, Spain). Neues Jahrbuch für Geologie und Paläontologie Abhandlungen 159, 225–255.

Jabaloy, A., 1993. La estructura de la región occidental de la Sierra de los Filabres (Cordilleras Béticas). vol. 9. Tierras del Sur, Universidad de Granada, Granada, Spain, pp. 1–261.

Jabaloy, A., Gómez-Pugnaire, M.T., Padrón-Navarta, J.A., López Sánchez-Vizcaíno, V., Garrido, C.J., 2015. Subduction- and exhumation-related structures preserved in metaserpentinites and associated metasediments from the Nevado–Filábride Complex (Betic Cordillera, SE Spain). Tectonophysics 644-645, 40–57.

Kirchner, K.L., Behr, W.M., Loewy, S., Stockli, D.F., 2016. Early Miocene subduction in the western Mediterranean: constraints from Rb-Sr multimineral isochron geochronology. Geochemistry, Geophysics, Geosystems 17. https://doi.org/10.1002/2015GC006208.

Kirkland, C.L., Smithies, H., Taylor, R., Evans, N.J., McDonald, B., 2015. Zircon Th/U ratios in magmatic environs. Lithos 212-215, 397–414.

Laborda-López, C., Aguirre, J., Donovan, S.K., 2013. Asociaciones de macrofósiles en rocas metamórficas del Complejo Nevado-Filábride (Zonas Internas de la Cordillera Bética) en Águilas, Murcia (SE España). Tafonomía y biocronoestratigrafía, XXIX Jornadas de Paleontología, pp. 83–84 Abstracts.

Laborda-López, C., Aguirre, J., Donovan, S.K., 2015a. Surviving metamorphism: taphonomy of fossil assemblages in marble and calc-silicate schist. PALAIOS 30, 668–679.

Laborda-López, C., Aguirre, J., Donovan, S.K., Navas-Parejo, P., Rodríguez, S., 2015b. Fossil assemblages and biochronology of metamorphic carbonates of the Nevado-Filábride Complex from the Águilas tectonic arc (SE Spain). Spanish Journal of Palaeontology 30, 275–292.

Lafuste, M.L.J., Pavillon, M.J., 1976. Mise en évidence d'Eifélien daté au sein des terrains métamorphiques des zones internes des Cordillères bétiques: Intérêt de ce nouveau repère stratigraphique. Comptes Rendus de l'Académie des Sciences de Paris 283, 1015–1018.

Linnemann, U., Gerdes, A., Drost, K., Buschmann, B., 2007. The continuum between Cadomian Orogenesis and opening of the Rheic Ocean: constraints from LA-ICP-MS U-Pb zircon dating and analysis of plate-tectonic setting (Saxo-Thuringian zone, NE Bohemian Massif, Germany). In: Linnemann, U., Nance, R.D., Kraft, P., Zulauf, G. (Eds.), The Evolution of the Rheic Ocean: From Avalonian–Cadomian Active Margin to Alleghenian-Variscan Collision: Boulder, Colorado. Geological Society of America Special Paper 423, pp. 61–96.

Linnemann, U., Pereira, F., Jeffries, T.E., Drost, K., Gerdes, A., 2008. The Cadomian Orogeny and the opening of the Rheic Ocean: the diachrony of geotectonic processes constrained by La-ICP-MS U-Pb zircon dating (Ossa-Morna and Saxo-Thuringian Zones, Iberian and Bohemian Massifs). Tectonophysics 461, 21–43.

Linnemann, U., Ouzegane, K., Drareni, A., Hofmann, M., Becker, S., Gärtner, A., Sagawe, A., 2011. Sands of West Gondwana: an archive of secular magmatism and plate interactions - a case study from the Cambro-Ordovician section of the Tassili Ouan Ahaggar (Algerian Sahara) using U-Pb-LA-ICP-MS detrital zircon ages. Lithos 123, 188–203.

López Sánchez-Vizcaino, V., Connolly, J.A.D., Gómez-Pugnaire, M.T., 1997. Metamorphism and phase relations in carbonate rocks from the Nevado-Filábride Complex (Cordilleras Béticas, Spain): application of the Ttn + Rt + Cal + Qtz + Gr buffer. Contributions to Mineralogy and Petrology 126, 292–302.

Margalef, A., Castiñeiras, P., Casas, J.M., Navidad, M., Liesa, M., Linnemann, U., Hofmann, M., Gärtner, A., 2016. Detrital zircons from the Ordovician rocks of the Pyrenees: geochronological constraints and provenance. Tectonophysics 681, 124–134.

Martínez Catalán, J.R., 2012. The Central Iberian arc, an orocline centered in the Iberian Massif and some implications for the Variscan belt. International Journal of Earth Sciences 101, 1299–1314.

Martínez Catalán, J.R., 2011. Are the oroclines of the Variscan belt related to late Variscan strike-slip tectonics? Terra Nova 23 (4), 241–247.

Martínez, F.J., Dietsch, C., Aleinikoff, J., Cirés, J., Arboleya, M.L., Reche, J., Gómez-Gras, D., 2016. Provenance, age, and tectonic evolution of Variscan flysch, southeastern France and northeastern Spain, based on zircon geochronology. Geological Society of America Bulletin 128, 842–859.

Martínez-Martínez, J.M., 1986. Evolución tectono-metamórfica del Complejo Nevado-Filábride en el sector entre Sierra Nevada y Sierra de los Filabres (Cordilleras Béticas). Cuadernos de Geología de la Universidad de Granada 13, 1–194.

Meijninger, B.M.L., Vissers, R.L.M., 2007. Thrust-related extension in the Prebetic (southern Spain) and closure of the North Betic Strait. Revista de la Sociedad Geológica de España 20, 153–171.

Meinhold, G., Morton, A.C., Fanning, C.M., Frei, D., Howard, J.P., Phillips, R.J., Strogen, D., Whitham, A.G., 2011. Evidence from detrital zircons for recycling of Mesoproterozoic and Neoproterozoic crust recorded in Paleozoic and Mesozoic sandstones of southern Libya. Earth and Planetary Science Letters 312, 164–175.

Meinhold, G., Morton, A.C., Avigad, D., 2013. New insights into peri-Gondwana paleogeography and the Gondwana super-fan system from detrital zircon U–Pb ages. Gondwana Research 23:661–665. https://doi.org/10.1016/j.gr.2012.05.003.

Mezger, K., Krogstad, E.J., 1997. Interpretation of discordant U-Pb zircon ages: an evaluation. Journal of Metamorphic Geology 15, 127–140.

Möller, A., O'Brien, P.J., Kennedy, A., Kröner, A., 2003. Linking growth episodes of zircon and metamorphic textures to zircon chemistry: an example from the ultrahigh-temperature granulites of Rogaland (SW Norway). In: Vance, D., Müller, W., Villa, I.M. (Eds.), Geochronology: Linking the Isotopic Record with Petrology and Textures. Geological Society of London, Special Publications vol. 220, pp. 65–81.

Nance, R.D., Murphy, J.B., 1994. Contrasting basement isotopic signatures and the palinspastic restoration of peripheral orogens: example from the Neoproterozoic Avalonian–Cadomian belt. Geology 22, 617–620.

Nasdala, L., Hofmeister, W., Norberg, N., Mattinson, J.M., Corfu, F., Dörr, W., Kamo, S.L., Kennedy, A.K., Kronz, A., Reiners, P.W., Frei, D., Košler, J., Wan, Y., Götze, J., Häger, T., Kröner, A., Valley, J.W., 2008. Zircon M257 - a homogeneous natural reference material for the ion microprobe U-Pb analysis of zircon. Geostandards and Geoanalytical Research 32, 247–265.

Nasdala, L., Reiners, P.W., Garver, J.I., Kennedy, A.K., Stern, R.A., Balan, E., Wirth, R., 2004. Incomplete retention of radiation damage in zircon from Sri Lanka. American Mineralogist 89, 219–231.

Oliveira, J.T., Horn, M., Paproth, E., 1979. Preliminary note on the stratigraphy of the Baixo Alentejo Flysch Group, Carboniferous of southern Portugal and on the palaeographic development, compared to corresponding units in Northwest Germany. Comunicações dos Serviços Geológicos de Portugal 65, 151–168.

Padrón-Navarta, J.A., López Sánchez-Vizcaíno, V., Garrido, C.J., Gómez-Pugnaire, M.T., 2011. Metamorphic record of high-pressure dehydration of antigorite Serpentinite to chlorite Harzburgite in a subduction setting (Cerro del Almirez ultramafic massif, Nevado-Filábride complex, S. Spain). Journal of Petrology 52:2047–2078. https://doi.org/10.1093/petrology/egr039.

Pastor-Galán, D., Gutiérrez-Alonso, G., Murphy, J.B., Fernández-Suárez, J., Hoffman, M., Linnemann, U., 2013. Provenance analysis of the Paleozoic sequences of the northern Gondwana margin in NW Iberia: passive margin to Variscan collision and orocline development. Gondwana Research 23, 1089–1103.

Paton, C., Hellstrom, J., Paul, B., Woodhead, J., Hergt, J., 2011. Iolite: freeware for the visualisation and processing of mass spectrometric data. Journal of Analytical Atomic Spectrometry 26, 2508–2518.

Pereira, M.F., Chichorro, M., Johnston, S.T., Gutiérrez-Alonso, G., Silva, J.B., Linnemann, U., Hofmann, M., Drost, K., 2012. The missing Rheic Ocean magmatic arcs: provenance analysis of Late Paleozoic sedimentary clastic rocks of SW Iberia. Gondwana Research 3–4 (22), 882–891.

Pereira, M.F., Ribeiro, C., Vilallonga, F., Chichorro, M., Drost, K., Silva, J.B., Albardeiro, L., Hofmann, M., Linnemann, U., 2014. Variability over time in the sources of South Portuguese Zone turbidites: evidence of denudation of different crustal blocks during the assembly of Pangaea. International Journal of Earth Sciences 103, 1453–1470.

Perrone, V., Martín-Algarra, A., Critelli, S., Decandia, F.A., D'Errico, M., Estévez, A., Iannace, A., Lazarrotto, A., Martín-Martín, M., Martín-Rojas, I., Mazzoli, S., Messana, A., Mongelli, G., Vitale, S., Zaghloul, M., 2006. Verrucano and Pseudoverrucano in the central-western Mediterranean Alpine chains: palaeogeographic evolution and geodynamic significance. In: Moratti, G., Chalouan, A. (Eds.), Tectonics of the Western Mediterranean and North Africa. Geological Society of London Special Publication Vol. 262, pp. 1–43.

Platt, J.P., Allerton, S., Kirker, A., Mandeville, C., Mayfield, A., Platzman, E.S., Rimi, A., 2003. The ultimate arc: differential displacement, Oroclinal bending, and vertical axis rotation in the external Betic-Rif arc. Tectonics 22 (3), 1017.

Platt, J.P., Anczkiewicz, R., Soto, J.I., Kelley, S.P., Thirlwall, M., 2006. Early Miocene continental subduction and rapid exhumation in the western Mediterranean. Geology 34, 981–984.

Platt, J.P., Behr, W.M., Johanesen, K., Williams, J.R., 2013. The Betic-Rif arc and its orogenic hinterland: a review. Annual Review of Earth Planetary Sciences 41:14.1–14.45. https://doi.org/10.1146/annurev-earth-050212-123951.

Puga, E., Diaz De Federico, A., Fontbote, J.M., 1974. Sobre la individualización y sistematización de las unidades profundas de la Zona Bética. Estudios Geológicos 30, 543–548.

Puga, E., Díaz De Federico, A., Nieto, J.M., 2002. Tectonostratigraphic subdivision and petrological characterisation of the deepest complexes of the Betic zone: a review. Geodinamica Acta 15, 23–43.

Rejebian, V.A., Harris, A.O., Huebner, J.S., 1987. Conodont color and textural alteration: an index to regional metamorphism, contact metamorphism, and hydrothermal alteration. Geological Society of America Bulletin 99, 471–479.

Rodrigues, B., Chew, D.M., Jorge, R.C.G.S., Fernandes, P., Veiga-Pires, C., Oliveira, J.T., 2015. Detrital zircon geochronology of the Carboniferous Baixo Alentejo Flysch Group (South Portugal); constraints on the provenance and geodynamic evolution of the South Portuguese Zone. Journal of the Geological Society, London 172, 294–308.

Rodriguez-Cañero, R., Jabaloy-Sánchez, A., Navas-Parejo, P., Martín-Algarra, A., 2018. Linking Palaeozoic palaeogeography of the Betic Cordillera to the Variscan Iberian Massif: new insight through the first conodonts of the Nevado-Filábride complex. International Journal of Earth Sciences 107 (5):1791–1806. https://doi.org/10.1007/s00531-017-1572-8.

Rodríguez-Fernández, L.R., 1994. La estratigrafía del Paleozoico y la estructura de la región de Fuentes Carrionas y áreas adyacentes (Cordillera herciniana, NO de España). Laboratorio Xeolóxico de Laxe, Serie Nova Terra, La Coruña, Spain 240 pp.

Roep, T.B., 1972. Stratigraphy of the "Permo-Triassic" Saladilla formation and its tectonic setting in the Betic of Malaga (Vélez Rubio region, SE Spain). Proceedings of the Koninklijke Nederlandse Akademie van Wetenschappen 75, 223–247.

Rubatto, D., Gebauer, D., 2000. Use of cathodoluminescence for U-Pb Zircon dating by ion microprobe: some examples from the Western Alps. In: Pagel, M., Barbin, V., Blanc, P., Ohnenstetter, D. (Eds.), Cathodoluminescence in Geosciences. Springer Verlag, Berlin, pp. 373–400.

Sánchez Martínez, S., De la Horra, R., Arenas, R., Gerdes, A., Galán-Abellán, A.B., López-Gómez, J., Barrenechea, J.F., Arche, A., 2012. U-Pb ages of detrital zircons from the Permo-Triassic series of the Iberian ranges: a record of variable provenance during rift propagation. The Journal of Geology 120, 135–154.

Sánchez-Martínez, S., Arenas, R., García, F.D., Martínez-Catalán, J.R., Gómez-Barreiro, J., Pearce, J.A., 2007. Careon ophiolite, NW Spain: suprasubduction zone setting for the youngest Rheic Ocean floor. Geology 35, 53–56.

Santamaría-López, A., Sanz De Galdeano, C., 2018. SHRIMP U–Pb detrital zircon dating to check subdivisions in metamorphic complexes: a case of study in the Nevado–Filábride complex (Betic Cordillera, Spain). International Journal of Earth Sciences https://doi.org/10.1007/s00531-018-1613-y.

Sanz-López, J., Blanco Ferrera, S., 2012. Lower Bashkirian conodonts from the Iraty Formation in the Alduides-Quinto Real Massif (Pyrenees, Spain). Geobios 45, 397–411.

Sanz-López, J., Blanco Ferrera, S., García-López, S., Sánchez De Posada, L.C., 2006. The mid-Carboniferous boundary in northern Spain: difficulties for correlation of the global stratotype section and point. Rivista Italiana di Paleontologia e Stratigrafia 112, 3–22.

Sláma, J., Košler, J., Condon, D.J., Crowley, J.L., Gerdes, A., Hanchar, J.M., Horstwood, M.S.A., Morris, G.A., Nasdala, L., Norberg, N., Schaltegger, U., Schoene, B., Tubrett, M.N., Whitehouse, M.J., 2008. Plešovice zircon - a new natural reference material for U–Pb and Hf isotopic microanalysis. Chemical Geology 249, 1–35.

Stampfli, G.M., Hochard, C., Vérard, C., Wilhem, C., von Raumer, J., 2013. The formation of Pangea. Tectonophysics 593, 1–19.

Stampfli, G.M., Kozur, H., 2006. Europe from the Variscan to the Alpine cycles. In: Gee, D.G., Stephenson, R. (Eds.), European Lithosphere Dynamics. Geological Society, London, Memoir Vol. 32, pp. 57–82.

Trommsdorff, V., López Sánchez-Vizcaíno, V., Gómez-Pugnaire, M.T., Müntener, O., 1998. High pressure breakdown of antigorite to spinifex-textured olivine and orthopyroxene, SE Spain. Contributions to Mineralogy and Petrology 132, 139–148.

Vai, G.B., Boriani, A., Rivalenti, G., Sassi, F.P., 1984. Catena ercinica e Paleozoico nelle Alpi Meridionali. Cento Anni di Geologia Italiana. Vol. Giub. I. Centenario SGI, Bologna, pp. 133–154.

Vissers, R.L.M., 1981. A structural study of the Central Sierra de los Filabres (Betic Zone, SE Spain), with emphasis on deformational process and their relation to the Alpine Metamorphism. GUA Papers on Geology, Series 1, 15 (154 pp).

Voet, H.W., 1967. Geological investigations in the Northern Sierra de Los Filabres around Macael and Cóbdar, southeastern Spain. Ph.D. Thesis. Amsterdam University, The Netherlands.

von Raumer, J., Stampfli, G.M., 2008. The birth of the Rheic Ocean-early Palaeozoic subsidence patterns and tectonic plate scenarios. Tectonophysics 461, 9–20.

von Raumer, J., Stampfli, G.M., Arenas, R., Sánchez-Martínez, S., 2015. Ediacaran to Cambrian oceanic rocks of the Gondwana margin and their tectonic interpretation. International Journal of Earth Sciences 104, 1107–1121.

von Raumer, J., Nesbor, H.D., Stampfli, G.M., 2017. The north-subducting Rheic Ocean during the Devonian: consequences for the Rhenohercynian ore sites. International Journal of Earth Sciences 106 (7), 2279–2296.

Wagner, R.H., Winkler Prins, C.F., Riding, R.E., 1971. Lithostratigraphic units of the lower part of the Carboniferous in northern León, Spain. Trabajos de Geología, Universidad de Oviedo 4, 603–663.

Wiedenbeck, M., Allé, P., Corfu, F., Griffin, W.L., Meier, M., Oberli, F., von Quadt, A., Ruddick, J.C., Spiegel, W., 1995. Three natural zircon standards for U-Th-Pb, Lu-Hf, trace element and REE analyses. Geostandards Newsletter 19, 1–23.

Williams, I.S., Claesson, S., 1987. Isotopic evidence for the Precambrian provenance and Caledonian metamorphism of high grade paragneisses from the Seve Nappes, Scandinavian Caledonides. II: Ion microprobe zircon U-Th-Pb. Contributions to Mineralogy and Petrology 97, 205–217.